Orientational correlations and spin relaxation in lamellar fluid membrane phases

Bertil Halle and Stefan Gustafsson
Condensed Matter Magnetic Resonance Group, Department of Chemistry, Lund University, P.O. Box 124, S-22100 Lund, Sweden
(Received 10 July 1996; revised manuscript received 24 March 1997)

Thermal fluctuations of fluid membranes in multilamellar systems have been extensively studied during the past decade by means of nuclear spin relaxation. Such data have generally been analyzed in terms of an effectively two-dimensional membrane model, which does not properly incorporate the mutual coupling of the individual membranes. Here we present a comprehensive theory of spin relaxation induced by small-amplitude, long-wavelength elastic distortions in a multilamellar stack of fluid membranes. In contrast to previous theoretical treatments, we find that membrane coupling can profoundly affect the spin relaxation behavior via its effect on the amplitudes and rates of membrane distortion modes. A physical basis for the resulting, rather intricate, spin relaxation behavior is provided by analyzing the spatial correlation function for the local membrane orientation. We find that the decay of this function involves two correlation lengths: one is related to interactions with the two adjacent membranes, and the other reflects the coherent fluctuation modes in the entire membrane stack. This analysis explains why the time correlation function has the asymptotic form $1/\tau^2$ rather than $1/\tau$, as expected for a two-dimensional system. A reinterpretation of existing low-frequency spin relaxation data from multilamellar phospholipid-water dispersions in terms of our theory should provide valuable insights into the nature of intermembrane forces. [S1063-651X(97)03707-0]

PACS number(s): 68.10.−m, 61.30.Gd, 76.60.Es, 87.22.Bt

I. INTRODUCTION

Thermal fluctuations profoundly influence the static and dynamic properties of any unidimensionally periodic structure [1]. Since the pioneering work of Helfrich [2], thermal out-of-plane fluctuations of fluid membranes in multilamellar assemblies have been widely studied [3,4]. Much of this work has focused on phospholipid membranes and the biological implications of membrane fluctuations. For the experimentalist, thermally induced membrane undulations provide a handle on two important microscopic properties: the bending rigidity of the membrane and the intermembrane force, which both affect the amplitude and rate of membrane undulations.

The technique of nuclear spin relaxation is arguably the most powerful probe of membrane undulations in multilamellar systems. The spin relaxation rate is governed by orientational correlations, and therefore reflects the spatial and temporal variation of thermally induced membrane curvature. While the static nuclear magnetic resonance line shape from a lamellar phase depends on the orientational fluctuations of the membranes [5], the adiabatic relaxation rate depends on their positional fluctuations [6]. The orientational fluctuations are governed by relatively short-wavelength undulation modes, and therefore mainly provide information about the bending rigidity. The positional fluctuations are influenced by long-wavelength modes and therefore also depend on the spatial variation of the intermembrane force. The intriguing possibility of using nuclear spin relaxation to study intermembrane forces has only recently been recognized [6].

Spin relaxation rates from multilamellar fluid membrane systems have been determined over a wide frequency range using field-cycling [7–9] or pulse-train [10–14] techniques, and at zero frequency using transverse relaxation [10–17]. All frequency-dependent relaxation data from multilamellar systems published to date have been interpreted in terms of a simple $1/\omega$ dispersion law. This dispersion law was first derived by Blinc *et al.* in connection with spin relaxation studies of a thermotropic smectic-*A* phase, for which it was concluded that undulation modes do not contribute significantly to the measured relaxation dispersion [18]. With multilamellar fluid membrane systems in mind, Marqusee, Warner, and Dill later rederived the $1/\omega$ law, obtaining a different prefactor [19]. Although this derivation is based on the undulation mode spectrum of a free membrane, it has been extensively applied to multilamellar systems under the assumption that membrane coupling can be ignored [19].

The extant theoretical treatments of the adiabatic spectral density that governs transverse spin relaxation are also based on the undulation mode spectrum of a free membrane, but differ in the dispersion relation adopted for the mode decay rate [11,20]. Stohrer *et al.* [11] used the $q_\perp^2$ dispersion appropriate for a purely transverse undulation mode ($q_\perp$ is the magnitude of a wavevector in the membrane plane). Bloom and Evans [20] advocated either a free-membrane $q_\perp^3$ dispersion or a ''red-blood-cell'' $q_\perp^6$ dispersion appropriate for a pair of membranes fluctuating under the constraint of constant enclosed volume [21]. These three dispersion relations differ solely in the way hydrodynamic interaction is taken into account. All of them ignore direct membrane coupling. To avoid divergences in these treatments, the elastic mode spectrum must be truncated. This transverse cutoff length has been variously referred to as ''a long-wavelength cutoff for the elastic modes'' (of unspecified physical origin) [11–13], a magnetic coherence length [14], or an effective correlation length for membrane undulations [20].

In a recent, more rigorous treatment of spin relaxation in multilamellar systems [6], membrane coupling was incorporated at the ouset in the elastic Hamiltonian [22]. The adiabatic spectral density differs qualitatively from previous re-

sults [11,20], and there is no need for a transverse cutoff. Moreover, while a $1/\omega$ dispersion regime also emerges from the coupled theory, it occurs well above the experimental frequency window. Since the experimental relaxation dispersions do exhibit a $1/\omega$ regime, they might seem to contradict the coupled theory. As stressed in previous work [6], however, the mode dispersion was taken to be of the $q_\perp^2$ form. The results in Ref. [6] are therefore strictly valid only when molecular diffusion along the membrane is much faster than membrane undulation. In the opposite limit (and in the general case), it is necessary to take membrane coupling into account not only in the static mode spectrum, but also in the dynamics of elastic modes [22,23].

In this work, we present a comprehensive theory of spin relaxation induced by small-amplitude, long-wavelength elastic distortions in a multilamellar stack of fluid membranes, a relaxation mechanism referred to in the literature as order director fluctuations or membrane undulations. The present theory differs from previous treatments of the same problem primarily in that we include membrane coupling in a consistent way in the static as well as dynamic properties. Although the underlying continuum description of the elastic distortions and the hydrodynamics of a lamellar phase rests on a firm foundation [22], the involvement of six distinct length scales makes the problem intricate and sometimes subtle.

The outline and principal results of the paper are as follows. Section II serves to establish a convenient notation for the subsequent development, and to make explicit the connection between the experimental observables and the central objects of the theory, the orientational time correlation function $G(\tau)$, and the corresponding spectral density function $J(\omega)$. Since the theory is restricted to the harmonic regime of small fluctuations, we consider only the correlation function that is of second order in the membrane displacement gradient.

Having introduced the two elastic modulii that govern membrane fluctuations in a lamellar phase (Sec. III), we consider in some detail the spatial correlation function $H_\perp(r_\perp)$ for the orientation of the projected local membrane normals (Sec. IV). The relative importance of bending rigidity and membrane coupling is gauged by the so-called patch length ξ_K, which emerges naturally from the free energy of elastic deformation of a multilamellar assembly, but does not appear in the single-membrane approach. First implicit in the work of Helfrich on steric interactions in multilamellar systems [24,25], the patch length defines the crossover from a short-wavelength regime with independent membrane fluctuations to a long-wavelength regime with coupled fluctuations [26–29]. It is then natural to assume that $H_\perp(r_\perp)$ decays more or less exponentially on the scale of ξ_K [26]. We find, however, that while $H_\perp(r_\perp)$ has indeed decayed to zero at $r_\perp \approx \xi_K$, the membrane normals remain weakly (anti) correlated over much longer distances. Consequently, two correlation lengths are needed to characterize the decay of $H_\perp(r_\perp)$. This finding explains why, in the diffusion limit, $G(\tau)$ decays asymptotically as $1/\tau^2$ rather than as $1/\tau$, as is usually the case for diffusion in unbounded two-dimensional systems [30–32].

In Sec. V, we investigate the effect of an external magnetic field on membrane fluctuations. Whereas the magnetic torque radically changes the fluctuations of a free membrane, it is strongly opposed by membrane coupling in a multilamellar system. For practical purposes, the magnetic-field effect on $J(\omega)$ can therefore often be ignored, and is not likely to be responsible for the low-frequency plateau in $J(\omega)$ [33]. This situation may be contrasted with that in nematic phases, where the magnetic field plays a more importance role due to the longer range $(1/r)$ of the orientational correlations [22] and the absence of a compressional restoring force. Not only does the external magnetic field influence the adiabatic spectral density $J(0)$, it can also break the symmetry of a uniaxial nematic phase, modifying the orientation dependence of the spin relaxation rates [34].

The time correlation function $G(\tau)$ reflects temporal fluctuations of the local membrane orientation at the location of the spin-bearing molecule. These fluctuations can result from molecular self-diffusion along the curved membrane or from membrane undulation dynamics. In Sec. VI, we discuss these two processes. Membrane coupling has a profound effect on both static and dynamic aspects of the elastic distortions in a lamellar phase. The static effect is due to the spatial constraint imposed by intermembrane repulsion on the amplitude of membrane fluctuations. The dynamic effect, which may be even more important, arises because membrane coupling induces coherent displacement fluctuations in the membrane stack [22,23]. Since these coherent fluctuations are much slower than purely transverse membrane undulation modes, they produce a dispersion in $J(\omega)$ at much lower frequencies than in the absence of membrane coupling.

The principal results of this work are contained in Secs. VII and VIII, where we calculate the time correlation function $G(\tau)$ and spectral density function $J(\omega)$. In Sec. VII we consider the limit where molecular diffusion is much faster than membrane undulation. This limit is at least approximately realized for mobile counterions in oil-swollen dilute lamellar phases [5]. Since it admits a fully analytical treatment, this limiting case is also of considerable heuristic value, providing physical insights not so easily gleaned from a numerical treatment. While the spectral density $J(\omega)$ in the fast-diffusion limit was presented in a preliminary report [6], the presentation in Sec. VII goes further by considering also the time correlation function $G(\tau)$. In particular, we relate the asymptotic decay of $G(\tau)$ for finite and infinite systems to the peculiar behavior of the orientational correlation function $H_\perp(r_\perp)$. We also show that the $1/\omega$ dispersion law [18,19] applies only at frequencies $\omega \gg \omega_K^S$, where $1/\omega_K^S$ sets the time scale for diffusion out of the initial membrane patch of area ξ_K^2, where membrane coupling is not manifested.

In Sec. VIII, we treat the general case where both molecular diffusion and membrane undulation contribute to the temporal fluctuations. When diffusion is slow compared to undulation, as for phospholipid membranes, the dynamic coupling effect is dramatically manifested in $J(\omega)$ at low frequencies. An analytical result is obtained for $J(0)$, revealing an extremely strong dependence on membrane coupling in the slow-diffusion limit: $J(0) \propto \xi_K^6$ as compared to $J(0) \propto \xi_K^2$ in the fast-diffusion limit. If membrane coupling is strong, the $J(\omega)$ dispersion is essentially the same as in the diffusion limit, with a $1/\omega$ regime extending down to ω_K^C, where $1/\omega_K^C$ measures the time scale for membrane undula-

tions of wavelength ξ_K. If membrane coupling is weak (ξ_K much larger than the intermembrane spacing); however, the $1/\omega$ regime extends down to the diffusional frequency ω_K^S, which is a much lower frequency when diffusion is much slower than membrane undulation.

We believe that these results can account for the low-frequency spin relaxation behavior in multilamellar systems [7–17]. A detailed reanalysis of the experimental data in terms of the present theory, deferred to a subsequent publication, should provide valuable insights into the nature of intermembrane forces.

II. NUCLEAR SPIN RELAXATION IN A LAMELLAR PHASE

A. Spectral density functions

Within the regime of the conventional second-order perturbation theory of nuclear spin relaxation [35], the accessible information about the amplitudes and rates of the fluctuations that induce spin relaxation is contained in a set of irreducible crystal-frame spectral density functions [36,37]. In the absence of a symmetry-breaking external field (cf. Sec. V D), the lamellar phase is uniaxial (crystallographic point group $\mathcal{D}_{\infty h}$). There are then three irreducible spectral density functions

$$J^C_{nn}(\omega)=\int_0^\infty d\tau\,\cos(\omega\tau)G^C_{nn}(\tau)\quad (n=0,\ 1,\ \text{and}\ 2). \tag{2.1}$$

The corresponding irreducible time correlation functions are [35–37]

$$G^C_{nn}(\tau)=\langle C_{2n}[\theta(0),\phi(0)]C^*_{2n}[\theta(\tau),\phi(\tau)]\rangle - \delta_{n0}\langle P_2(\cos\theta)\rangle^2, \tag{2.2}$$

where the arguments of the (unnormalized) spherical harmonics $C_{2n}(\theta,\phi)$ specify the instantaneous orientation of the major principal axis of the spin-lattice coupling tensor with respect to a crystal-fixed frame (with the z axis along the optic axis of the lamellar phase).

The observable spin relaxation rates can usually be expressed as linear combinations of the crystal-frame spectral densities in Eq. (2.1). For a uniaxial phase [37],

$$J^L_{kk}(\omega_k;\beta)=\sum_{n=0}^{2}(1-\delta_{n0}/2)\{[d^2_{kn}(\beta)]^2 + [d^2_{k-n}(\beta)]^2\}J^C_{nn}(\omega_k), \tag{2.3}$$

where $d^2_{kn}(\beta)$ is a reduced Wigner function [38], and β is the angle between the optic axis and the external magnetic field. By recording the orientation (β) dependence of the spin relaxation rates, the model-independent quantities $J^C_{nn}(\omega_k)$ can be determined.

The dynamic processes responsible for spin relaxation in a lamellar phase take place on a broad timescale. Local molecular motions, such as conformational dynamics and restricted molecular reorientation, dominate the relaxation in the conventional range of Larmor frequencies ($\omega_0/2\pi \approx 1-100$ MHz) [39]. Here we are concerned with collective orientational fluctuation modes that, due to their small amplitude, contribute significantly to spin relaxation only if they are much slower than the local molecular motions. Such director fluctuations are therefore important only at frequencies much lower than the conventional MHz range [8].

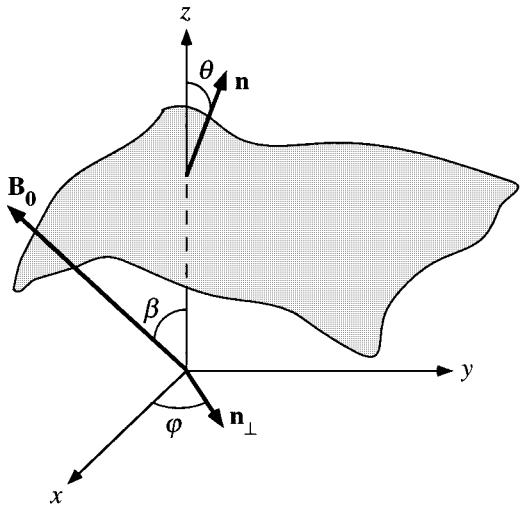

FIG. 1. A patch of membrane, showing the definitions of the director **n**, its projection $\mathbf{n}_\perp$ on the x-y base plane, and the angles θ, φ and β. The x axis is defined so that the external magnetic field $\mathbf{B}_0$ is in the x-z plane.

In field-cycling relaxation experiments, all three lab-frame spectral density functions $J^L_{kk}(\omega_k;\beta)$ provide information about director fluctuations, since the probing frequency ω_k can be varied over a wide range, down to ~ 1 kHz [40]. At conventional Larmor frequencies (MHz range), director fluctuations contribute only to the secular lab-frame spectral density function $J^L_{00}(\omega;\beta)$, which is probed at zero frequency by the transverse relaxation rate (or the homogeneous linewidth) and in the kHz range by pulse-train experiments. In particular, the Carr-Purcell-Meiboom-Gill spin-echo experiment measures an effective spectral density function [41]

$$J^L_{\mathrm{CPMG}}(\omega;\beta)=\frac{8}{\pi^2}\sum_{p=0}^{\infty}(2p+1)^{-2}J^L_{00}[(2p+1)\pi\omega/2;\beta], \tag{2.4}$$

where ω now denotes the pulse-train frequency.

B. Small-amplitude director fluctuations

In the frequency range where director fluctuations contribute significantly to spin relaxation, the much faster local motions are manifested as a frequency-independent additive contribution to the crystal-frame spectral density functions. The director fluctuation contribution is then described by Eq. (2.2), where the angles (θ,ϕ) now specify the orientation of the local membrane normal, referred to as the director **n**, with respect to the optic axis (cf. Fig. 1). (The faster molecular motions also renormalize the spin-lattice coupling constant, the square of which multiplies the spectral densities, as defined here, in the expressions for spin relaxation rates [37].)

The time correlation functions in Eq. (2.2) may be expressed in terms of the projection $\mathbf{n}_\perp$ of the director on the

base plane (orthogonal to the optic axis) as

$$G_{00}^{C}(\tau)=O(n_{\perp}^{4}), \tag{2.5a}$$

$$G_{11}^{C}(\tau)=\tfrac{3}{2}\langle \mathbf{n}_{\perp}(0)\cdot\mathbf{n}_{\perp}(\tau)\rangle+O(n_{\perp}^{4}), \tag{2.5b}$$

$$G_{22}^{C}(\tau)=O(n_{\perp}^{4}). \tag{2.5c}$$

If the director fluctuations are of small amplitude, i.e., if the director does not deviate much from the optic axis so that $\langle n_{\perp}^{2}\rangle \ll 1$, we may neglect fourth-order and higher contributions to Eq. (2.5). Director fluctuations are then manifested exclusively via the second-order time correlation function $G_{11}^{C}(\tau)$ and the corresponding crystal-frame spectral density function $J_{11}^{C}(\omega)$. The latter contributes to the secular lab-frame spectral density function (which is probed at low frequencies) according to Eq. (2.3):

$$J_{00}^{L}(\omega;\beta)=\tfrac{9}{2}\sin^{2}\beta\,\cos^{2}\beta\,J(\omega), \tag{2.6}$$

where, for notational convenience, we defined the second-order crystal-frame spectral density function

$$J(\omega)=\int_{0}^{\infty} d\tau\,\cos(\omega\tau)G(\tau), \tag{2.7}$$

and the corresponding time correlation function

$$G(\tau)=\langle \mathbf{n}_{\perp}(0)\cdot\mathbf{n}_{\perp}(\tau)\rangle. \tag{2.8}$$

According to Eq. (2.6), the second-order director fluctuation contribution vanishes at the orientations $\beta=0$ and $\pi/2$, and goes through a maximum at $\beta=\pi/4$. At the former two orientations, therefore, the fourth-order contributions come into play. These are treated elsewhere [42].

C. Director fluctuations versus membrane undulations

In a continuum description, the configurational state of a uniaxial phase can be specified by a unit vector field $\mathbf{n}(\mathbf{r})$, giving at each point in space the orientation of the director with respect to the optic axis. This is the conventional description for nematic phases [22,43]. For lamellar phases, however, the configurational state is more naturally described in terms of a scalar field $u(\mathbf{r})$ (cf. Fig. 1), giving at each point the vertical (along the optic axis) membrane displacement away from a reference plane (the base plane) [22,44]. The displacement field $u(\mathbf{r})$ uniquely specifies a given thermally excited configuration of the multilamellar assembly with respect to the ''zero-temperature'' ground state of equidistant, flat membranes ($u\equiv 0$).

As long as the membranes are free from overhangs, so that a given membrane surface can be specified in the Monge representation $z=u(x,y)$, there is a unique one-to-one correspondence between the director and displacement fields [45],

$$\mathbf{n}=(\mathbf{n}_{\perp},n_{z})=\frac{(-\boldsymbol{\nabla}_{\perp}u,1)}{(1+|\boldsymbol{\nabla}_{\perp}u|^{2})^{1/2}}, \tag{2.9}$$

where $\boldsymbol{\nabla}_{\perp}=(\partial/\partial x,\partial/\partial y)$ is the transverse gradient operator. This exact relationship reflects the fact that a nonuniform displacement of a membrane necessarily induces curvature and, hence, a deflection of the director $\mathbf{n}$ away from the optic axis (0,0,1). To second order in the director fluctuation, Eq. (2.9) reduces to

$$\mathbf{n}_{\perp}=-\boldsymbol{\nabla}_{\perp}u. \tag{2.10}$$

It follows from Eqs. (2.9) or (2.10) that the descriptions of the motions that induce low-frequency spin relaxation in multilamellar systems as ''order director fluctuations'' (modulation of $\mathbf{n}$) or as ''membrane undulations'' (nonuniform modulation of u) are entirely equivalent. This fundamental duality is apparently not generally appreciated [14,16,17]. Indeed, some authors treat director fluctuations and membrane undulations as distinct relaxation mechanisms [16]. Here we use the two expressions ''director fluctuation'' and ''membrane undulation'' synonymously.

In the present work, we adopt the conventional view that the local membrane normal defines the preferred orientation of the constituent molecules. Moreover, we assume that the molecular orientation relaxes to the local uniaxial equilibrium distribution ''instantaneously'' on the time scale of membrane undulation and molecular diffusion. This is clearly not the case on molecular length scales, but it should be a valid description for the long-wavelength modes that dominate the low-frequency spin relaxation rate. Without this time-scale separation, the irreducible time correlation functions in Eq. (2.2) would have a more complicated structure, as used for describing the faster local motions responsible for spin relaxation in the MHz regime [46]. When the time scales are distinct, the faster motions only enter as a molecular order parameter, the square of which multiplies all spectral densities in the final expressions for the relaxation rates.

In lyotropic liquid crystals, the hydrophobically self-assembled amphiphilic aggregates introduce a supermolecular level of structural organization, allowing long-wavelength fluctuations to be described in terms of interface geometry. In molecular thermotropic liquid crystals this supermolecular level is absent, and the director $\mathbf{n}$ refers to a molecule-fixed axis rather than to the local interface normal. The order director fluctuation mechanism discussed for the molecular smectic-*A* phase [18,47,48] is therefore distinct from that considered here. In fact, the same viscoelastic continuum description has been used for molecular smectic-*A* and nematic phases [47–49]. A different continuum description has been employed near the (second-order) phase transition where critical fluctuations couple smectic and molecular order [50,51]. Such critical phenomena are not expected to be important in lyotropic systems, where the lamellar to nematic phase transition is generally first order.

D. Orientational structure factor

For a system of macroscopic but finite volume V, the displacement field $u(\mathbf{r})$ can be developed in a Fourier series as

$$u(\mathbf{r})=\sum_{\mathbf{q}}\,\hat{u}(\mathbf{q})\exp(i\mathbf{q}\cdot\mathbf{r}), \tag{2.11a}$$

with (complex-valued) reciprocal-space mode amplitudes

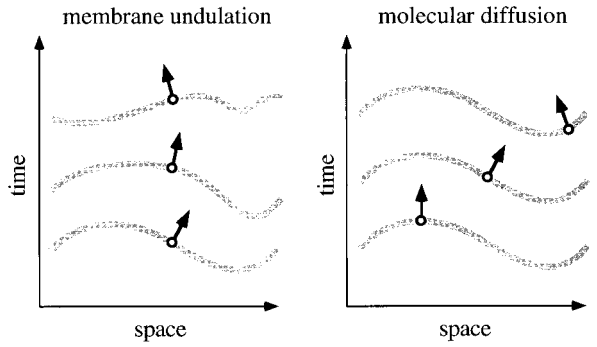

FIG. 2. Schematic illustration of the two dynamic processes that modulate the orientation of the membrane director **n** (arrows) in a lamellar phase: membrane undulation at a fixed position (left) and molecular diffusion on a frozen membrane (right).

$$\hat{u}(\mathbf{q}) = \frac{1}{V}\int d\mathbf{r}\; u(\mathbf{r})\exp(-i\mathbf{q}\cdot\mathbf{r}). \tag{2.11b}$$

Using Eqs. (2.10) and (2.11a), we can similarly expand the director field as

$$\mathbf{n}_\perp(\mathbf{r}) = -i\sum_{\mathbf{q}}\; \mathbf{q}_\perp \hat{u}(\mathbf{q})\exp(i\mathbf{q}\cdot\mathbf{r}), \tag{2.12}$$

with $\mathbf{q}_\perp = (q_x, q_y)$ the transverse wave vector.

The time correlation function $G(\tau)$ in Eq. (2.8) reflects temporal fluctuations of the director orientation experienced by the spin-bearing molecule. Two distinct dynamic processes can contribute to the time dependence of $\mathbf{n}_\perp(\tau)$ (cf. Fig. 2). A molecule that remains at a fixed position **r** experiences a time-dependent director due to thermally excited elastic distortions in the medium. If, on the other hand, the elastic distortions are frozen in, the molecule will still experience a time-dependent director due to its self-diffusion through the quenched director field. These two limiting cases correspond to an explicit time dependence $\mathbf{n}_\perp(\mathbf{r},\tau)$ and an implicit time dependence $\mathbf{n}_\perp(\mathbf{r}(\tau))$, respectively. In general, both processes take place simultaneously. If $\mathbf{n}_\perp$ is regarded as a function of τ, its Fourier decomposition should therefore be written

$$\mathbf{n}_\perp(\tau) = -i\sum_{\mathbf{q}}\; \mathbf{q}_\perp \hat{u}(\mathbf{q},\tau)\exp[i\mathbf{q}\cdot\mathbf{r}(\tau)]. \tag{2.13}$$

Inserting Eq. (2.13) into Eq. (2.8), we obtain

$$G(\tau) = \sum_{\mathbf{q}}\sum_{\mathbf{q}'}\; \mathbf{q}_\perp\cdot\mathbf{q}'_\perp \langle \hat{u}(\mathbf{q},0)\hat{u}^*(\mathbf{q}',\tau)\rangle_C \times \langle \exp\{i[\mathbf{q}\cdot\mathbf{r}(0) - \mathbf{q}'\cdot\mathbf{r}(\tau)]\}\rangle_S. \tag{2.14}$$

Here we assumed that collective elastic distortions (C) and molecular self-diffusion (S) are independent processes (cf. Sec. VI A), so that statistical (ensemble) averaging can be performed separately for each process. Next, we note that coupling of different **q** modes can be neglected in a macroscopic system [22], i.e.,

$$\langle \hat{u}(\mathbf{q},0)\hat{u}^*(\mathbf{q}',\tau)\rangle_C = \delta_{\mathbf{q},\mathbf{q}'}\langle \hat{u}(\mathbf{q},0)\hat{u}^*(\mathbf{q},\tau)\rangle_C, \tag{2.15}$$

whereby

$$G(\tau) = \sum_{\mathbf{q}}\; q_\perp^2 \langle \hat{u}(\mathbf{q},0)\hat{u}^*(\mathbf{q},\tau)\rangle_C \times \langle \exp\{-i\mathbf{q}\cdot[\mathbf{r}(\tau) - \mathbf{r}(0)]\}\rangle_S. \tag{2.16}$$

The last factor in Eq. (2.16) can be identified with the spatial Fourier transform, $F_S(\mathbf{q},\tau)$, of the single-particle translational diffusion propagator $F_S(\mathbf{r},\tau)$, i.e.,

$$F_S(\mathbf{q},\tau) = \langle \exp[-i\mathbf{q}\cdot\mathbf{r}(\tau)]\rangle_S = \frac{1}{V}\int d\mathbf{r}\; F_S(\mathbf{r},\tau)\exp(-i\mathbf{q}\cdot\mathbf{r}). \tag{2.17}$$

Note that we can set $\mathbf{r}(0) = \mathbf{0}$ in Eq. (2.16) without loss of generality, since the system is translationally invariant (all initial positions are statistically equivalent) on length scales where the continuum description holds. Furthermore, we introduce the (normalized) membrane displacement correlation function

$$F_C(\mathbf{q},\tau) = \langle \hat{u}(\mathbf{q},0)\hat{u}^*(\mathbf{q},\tau)\rangle_C / \langle |\hat{u}(\mathbf{q})|^2\rangle_C, \tag{2.18}$$

and the orientational structure factor

$$\hat{H}(\mathbf{q}) = q_\perp^2 \langle |\hat{u}(\mathbf{q})|^2\rangle_C, \tag{2.19}$$

which is the Fourier transform of the spatial orientational correlation function,

$$H(\mathbf{r}) = \langle \mathbf{n}_\perp(\mathbf{0})\cdot\mathbf{n}_\perp(\mathbf{r})\rangle_C = \sum_{\mathbf{q}}\; \hat{H}(\mathbf{q})\exp(i\mathbf{q}\cdot\mathbf{r}). \tag{2.20}$$

Combining Eqs. (2.16)–(2.19), we can express the time correlation function $G(\tau)$ on the compact form

$$G(\tau) = \sum_{\mathbf{q}}\; \hat{H}(\mathbf{q})F(\mathbf{q},\tau), \tag{2.21}$$

with

$$F(\mathbf{q},\tau) = F_C(\mathbf{q},\tau)F_S(\mathbf{q},\tau). \tag{2.22}$$

The spectral density function in Eq. (2.7) then becomes

$$J(\omega) = \sum_{\mathbf{q}}\; \hat{H}(\mathbf{q})S(\mathbf{q},\omega), \tag{2.23}$$

where $S(\mathbf{q},\omega)$ is the (normalized) dynamic orientational structure factor [52,53]

$$S(\mathbf{q},\omega) = \int d\tau\; \cos(\omega\tau)F(\mathbf{q},\tau). \tag{2.24}$$

III. ELASTIC DISTORTIONS IN A LAMELLAR PHASE

A. Free energy of elastic distortion

The phenomenological description of thermally excited elastic distortions in a lamellar phase, first developed for the smectic-*A* phase [22], is based on the energy functional

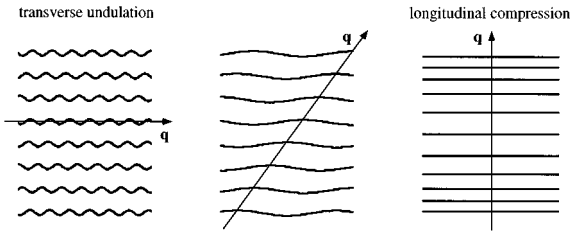

FIG. 3. The fundamental elastic distortion modes in a lamellar phase: the transverse undulation mode and the longitudinal compression mode. For transverse wavelengths $1/q_\perp$ shorter than ξ_K, the modes are incoherent, whereas, for longer wavelengths, there is a phase coherence between the membranes in the stack.

$$\mathcal{F}[u(\mathbf{r})]=\tfrac{1}{2}\int d\mathbf{r}\left[K_1(\nabla_\perp^2 u)^2+\overline{B}\left(\frac{\partial u}{\partial z}\right)^2\right], \tag{3.1}$$

where $\nabla_\perp^2=\partial^2/\partial x^2+\partial^2/\partial y^2$ is the transverse Laplacian and the integration is over the system volume V. This harmonic approximation is valid for weak fluctuations in the sense that $|\nabla u|^2=|\nabla_\perp u|^2+(\partial u/\partial z)^2\ll 1$. Equation (3.1) thus describes distortion modes of sufficiently long wavelengths that the membranes are only slightly tilted from the base plane and the spacing between successive pairs of membranes differs only slightly.

The lamellar phase is characterized by two macroscopic elastic modulii: K_1 is associated with director splay (or membrane bending) and $\overline{B}$ with longitudinal (along the optic axis) compression at constant chemical potential. The fundamental distortion modes associated with these elastic modulii are illustrated in Fig. 3. Since the pure compression mode does not introduce membrane curvature, it cannot affect the orientational correlation functions considered here. A general mode, however, is a mixture of the two fundamental modes. The first term in Eq. (3.1) is the harmonic approximation to the splay term $K_1(\nabla\cdot\mathbf{n})^2$ in the Oseen-Frank elastic free energy [43]. For a defect-free lamellar phase, the twist term vanishes identically, while the (director) bend term introduces a coupling between the two terms in Eq. (3.1), albeit of negligible magnitude [54].

To preserve full rotational invariance, $\partial u/\partial z$ should actually be replaced by $\partial u/\partial z-\frac{1}{2}|\nabla_\perp u|^2$ in Eq. (3.1). One effect of this anharmonic correction is to renormalize the elastic modulii K_1 and $\overline{B}$ [22,55]. For a lamellar phase in the harmonic regime, however, the elastic modulii are thus altered by at most a few percent.

B. Microscopic interpretation of elastic modulii

To relate the elastic modulii K_1 and $\overline{B}$ in the continuum description to microscopic structure and interactions, one notes that a lamellar phase is a stack of many discrete membranes. The configurational free energy of this system is taken to be of the form

$$\mathcal{F}=\sum_i \int d\mathbf{r}_\perp\{\tfrac{1}{2}\kappa H_i+[w(s_i)-w(d)]\}, \tag{3.2}$$

where $\mathbf{r}_\perp=(x,y)$, and the sum is taken over all membranes in the stack.

The first term in Eq. (3.2) is the Helfrich-Canham bending energy of a defect-free, symmetric bilayer membrane [56,57], with κ the bending rigidity and H_i the mean curvature of the ith membrane [45],

$$H_i=-\nabla_\perp\cdot\mathbf{n}_{\perp i}=\nabla_\perp^2 u_i+O[(\nabla_\perp u_i)^2], \tag{3.3}$$

where Eq. (2.9) was used in the last step.

The second term in Eq. (3.2) is the (free) energy of interaction per unit base area of two adjacent membranes with (local) separation s, relative to their interaction at the average membrane spacing d (the lamellar repeat distance). (Only nearest-neighbor interactions in the stack are included.) Since the separation between membranes i and $i+1$ is $s_i=d+u_{i+1}-u_i$, $w(s_i)$ may be expanded around $s_i=d$ as

$$w(s_i)-w(d)=w'(d)[u_{i+1}-u_i]+\tfrac{1}{2}w''(d)[u_{i+1}-u_i]^2+O([u_{i+1}-u_i]^3). \tag{3.4}$$

The linear term vanishes since, by definition, $w(s)$ is at a minimum for $s=d$.

The membrane is treated as an incompressible fluid layer of fixed thickness. The total membrane area in the sample is then a conserved quantity, unaffected by membrane undulations. The effect of shape fluctuations is simply to reduce the number of membranes in the sample, thereby increasing the mean membrane spacing d [4,5]. If membrane compression were allowed, Eq. (3.2) should be supplemented with an interfacial energy term [27].

Inserting the leading contributions of Eqs. (3.3) and (3.4) into Eq. (3.2) and passing to the continuum limit, with $(u_{i+1}-u_i)/d\to\partial u/\partial z$ and $d\Sigma_i\to\int dz$, we recover the harmonic continuum Hamiltonian, Eq. (3.1), with the identifications [58]

$$K_1=\kappa/d, \tag{3.5}$$

$$\overline{B}=dw''(d). \tag{3.6}$$

IV. ORIENTATIONAL CORRELATIONS IN A LAMELLAR PHASE

A. Transverse orientational correlations

With the aid of Eq. (2.11a), the harmonic free-energy functional (3.1) may be Fourier decomposed as [44]

$$\mathcal{F}[\{\hat{u}(\mathbf{q})\}]=\tfrac{1}{2}V\sum_{\mathbf{q}}(K_1 q_\perp^4+\overline{B}q_z^2)|\hat{u}(\mathbf{q})|^2. \tag{4.1}$$

Since the free energy is a sum of quadratic terms, the classical equipartition theorem tells us that the statistical average of each term equals $k_BT/2$. The orientational structure factor Eq. (2.15) thus becomes [44]

$$\hat{H}(\mathbf{q})=\frac{k_BT}{V}\frac{q_\perp^2}{K_1 q_\perp^4+\overline{B}q_z^2}. \tag{4.2}$$

The real-space orientational correlation function $H(\mathbf{r})$ can now be calculated by inserting Eq. (4.2) into Eq. (2.16). We shall be mainly interested in the transverse orientational cor-

relation function $H_\perp(\mathbf{r}_\perp)$ and the transverse orientational structure factor $\hat{H}_\perp(\mathbf{q}_\perp)$. These are interrelated through

$$H_\perp(\mathbf{r}_\perp)=\sum_{\mathbf{q}_\perp}\hat{H}_\perp(\mathbf{q}_\perp)\exp(i\mathbf{q}_\perp\cdot\mathbf{r}_\perp). \tag{4.3}$$

The transverse functions are related to their three-dimensional counterparts as

$$H_\perp(\mathbf{r}_\perp)=H(x,y,0), \tag{4.4}$$

$$\hat{H}_\perp(\mathbf{q}_\perp)=\frac{L_z}{2\pi}\int dq_z\hat{H}(\mathbf{q}). \tag{4.5}$$

The integration ranges in $\mathbf{q}$ space are $\pi/L_\perp\leqslant q_\perp\leqslant\pi/a$ in the base plane and $\pi/L_z\leqslant|q_z|\leqslant\pi/d$ along the optic axis. The low-wave-number cutoffs reflect the finite size of the sample (or homeotropic domain) of width $L_\perp$ and thickness L_z. The high-wave-number cutoffs acknowledge the breakdown of the continuum description on length scales comparable to the molecular width a and the mean membrane spacing d.

Converting the sum in Eq. (4.3) to an integral over $\mathbf{q}_\perp$ and integrating over the orientation of the $\mathbf{q}_\perp$ vector in the base plane, we obtain

$$H_\perp(r_\perp)=\frac{A}{2\pi}\int dq_\perp q_\perp\hat{H}_\perp(q_\perp)J_0(q_\perp r_\perp), \tag{4.6}$$

with A the base plane area and $J_0(x)$ the zeroth-order Bessel function. Next we calculate $\hat{H}_\perp(q_\perp)$ by inserting Eq. (4.2) into Eq. (4.5) and integrating over q_z:

$$\hat{H}_\perp(q_\perp)=\frac{k_BT\xi_K^2}{\pi A\kappa}\arctan\left[\frac{(q_\perp\xi_B)^2/\pi}{1+(q_\perp^2\xi_K\xi_B/\pi)^2}\right]. \tag{4.7}$$

Substituting this result into Eq. (4.6), the real-space orientational correlation function $H_\perp(r_\perp)$ is obtained after a numerical integration over $q_\perp$.

B. Correlation lengths

In Eq. (4.7), we introduced two transverse correlation lengths ξ_K and ξ_B, which characterize orientational correlations in a lamellar phase. They are defined as

$$\xi_K=(d^2K_1/\overline{B})^{1/4}, \tag{4.8}$$

$$\xi_B=(L_z^2K_1/\overline{B})^{1/4}. \tag{4.9}$$

The two correlation lengths are related through $\xi_B=N^{1/2}\xi_K$, with $N=L_z/d$ the number of membranes in the stack. With $N=10^4$, typical for a lamellar sample oriented between glass plates, ξ_B is thus two orders of magnitude larger than ξ_K. [In deriving Eq. (4.7), we also assumed that $N\gg1$.] Another relation is $\xi_B=(\lambda L_z)^{1/2}$, with $\lambda=(K_1/B)^{1/2}$ the so-called smectic penetration length [22]. With the aid of Eqs. (3.5) and (3.6), one obtains the microscopic relation $\xi_K=(\kappa/w''(d))^{1/4}$.

The physical significance of the correlation lengths may be appreciated with reference to Eq. (4.1), showing that the elastic free energy for a distortion mode of wave vector $\mathbf{q}$ is proportional to $K_1q_\perp^4+\overline{B}q_z^2$. For wave vectors such that $K_1q_\perp^4\gg\overline{B}q_z^2$ for all q_z within the range $\pi/L_z\leqslant|q_z|\leqslant\pi/d$, i.e., when $q_\perp\gg1/\xi_K$, we have essentially pure undulation modes, unaffected by membrane coupling. For wave vectors such that $K_1q_\perp^4\ll\overline{B}q_z^2$ for all q_z, i.e., when $q_\perp\ll1/\xi_B$, we have essentially pure compression modes, which do not induce membrane curvature. The correlation lengths ξ_K and ξ_B thus partition the transverse wavelength range into three regimes (cf. Fig. 3): an uncoupled, incoherent, short-wavelength regime ($1/q_\perp\ll\xi_K$), a coupled, intermediate-wavelength regime with phase coherence between the different membranes in the stack ($\xi_K<1/q_\perp<\xi_B$), and a long-wavelength compressional regime ($1/q_\perp\gg\xi_B$).

The correlation length ξ_K was first introduced within the context of sterically interacting membranes [24–26], where it can be loosely interpreted as the average distance between points of contact between adjacent membranes. In contrast to the positional correlation function $\langle u(\mathbf{0})u(\mathbf{r})\rangle$ and the associated positional structure factor probed by scattering experiments [59–62], the orientational correlation function $\langle\mathbf{n}_\perp(\mathbf{0})\cdot\mathbf{n}_\perp(\mathbf{r})\rangle$ probed by nuclear spin relaxation has apparently not been examined in detail previously. Presumably for this reason, the correlation length ξ_B has not been identified before.

The importance of ξ_B for spin relaxation in lamellar phases is readily appreciated. Since the fluctuation modes are of small amplitude in the harmonic regime, they make substantial contributions to spin relaxation only if they are slow, which means long wavelengths. However, modes of wavelengths exceeding ξ_B, although slow, have vanishing orientational amplitude since they are essentially compressional. The correlation length ξ_B thus acts as a transverse cutoff, beyond which no modes contribute significantly to orientational correlation functions or spin relaxation rates. Provided that $\xi_B\ll L_\perp$, the membrane size $L_\perp$ is therefore irrelevant. In contrast, since $\xi_B\propto L_z^{1/2}$, the thickness of the membrane stack does influence orientational fluctuations of long wavelengths and at low frequencies.

C. Orientational correlation for a free membrane

In the free-membrane limit ($\overline{B}=0$), Eq. (4.8) shows that ξ_K diverges, so that Eqs. (4.6) and (4.7) yield [26]

$$H_\perp(r_\perp)=\frac{k_BT}{2\pi\kappa}\int dq_\perp\frac{1}{q_\perp}J_0(q_\perp r_\perp)=\frac{k_BT}{2\pi\kappa}\ln\left(\frac{L_\perp}{\pi r_\perp}\right), \tag{4.10}$$

where $r_\perp\gg a/\pi$ was assumed in the last step. The mean-square director fluctuation of a free membrane is obtained by setting $r_\perp=0$ in the integrand of Eq. (4.10), with the result [2]

$$\langle n_\perp^2\rangle=H_\perp(0)=\frac{k_BT}{2\pi\kappa}\ln(L_\perp/a). \tag{4.11}$$

The logarithmically slow decay of the orientational correlation function (4.10) and the logarithmically divergent thermodynamic limit ($L_\perp\to\infty$) of the mean-square fluctuation (4.11) demonstrate that a free membrane does not possess

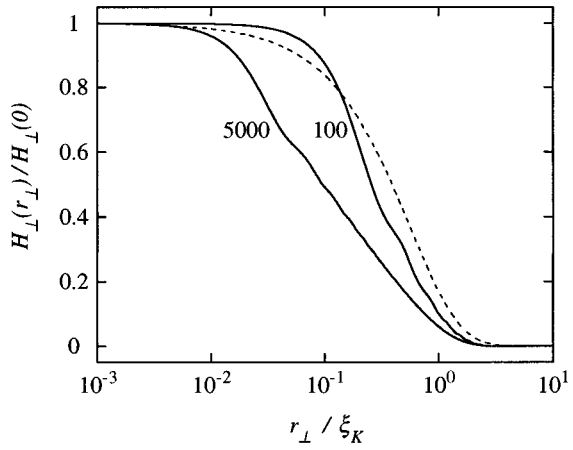

FIG. 4. Transverse orientational correlation function, $H_\perp(r_\perp)$, calculated from Eqs. (4.6) and (4.7) with $N=10^4$ and $\pi(\xi_K/a)^2$ values as indicated. The dashed curve shows an exponential correlation function with decay length $\xi_K/\pi^{1/2}$.

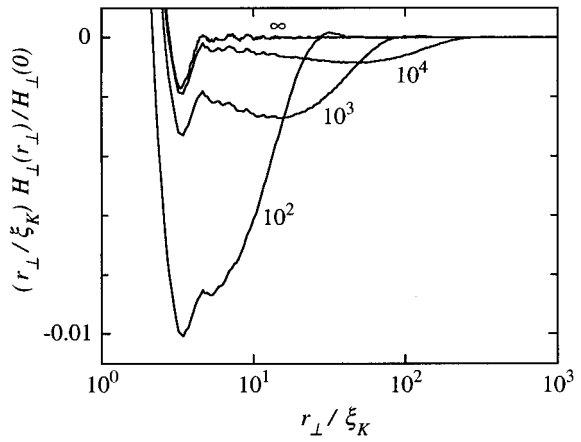

FIG. 5. Long-range behavior of the transverse orientational correlation function, $H_\perp(r_\perp)$, calculated from Eqs. (4.6) and (4.7) with $\pi(\xi_K/a)^2=5000$ and N values as indicated. To emphasize the weak, long-ranged tail in $H_\perp(r_\perp)$, it has been multiplied by $r_\perp$ (proportional to the area element in the base plane). The small-scale roughness results from the short-wavelength cutoff a.

true long-range orientational order [26,58]. While the harmonic approximation breaks down as $\langle n_\perp^2\rangle$ approaches unity, it can be shown that a free membrane, no matter how rigid locally (large κ), is crumpled on length scales larger than the free-membrane persistence length [26,58]

$$\xi_P = a\, \exp\left(\frac{4\pi\kappa}{3k_BT}\right). \tag{4.12}$$

For a relatively stiff membrane with $\kappa \gg k_BT$, as for a phospholipid bilayer, ξ_P is of astronomical dimensions.

D. Orientational correlation for coupled membranes

In contrast to a free membrane, a membrane that is coupled to its neighbors in a lamellar phase exhibits true long-range orientational order, i.e., the harmonic theory predicts a finite $\langle n_\perp^2\rangle$ even in the thermodynamic limit ($L_\perp, L_z \to \infty$). Equations (4.6) and (4.7) yield a closed-form result for $\langle n_\perp^2\rangle$ [5], which, in the physically relevant regime where $\xi_K \gg a$ and $\xi_B \ll L_\perp$, reduces to

$$\langle n_\perp^2\rangle = \frac{k_BT}{4\pi\kappa}\,[1+2\ln(\pi^{1/2}\xi_K/a)], \tag{4.13}$$

which is independent of sample size. It is of interest to compare this result with the corresponding one for a nematic phase. In the one-constant approximation [22],

$$\langle n_\perp^2\rangle_{\text{nematic}} = \frac{k_BT}{\pi^2 K}\, q_c\,, \tag{4.14}$$

where K is the elastic constant and q_c a continuum cutoff. Taking $q_c=\pi/d$, we see that the director fluctuation amplitude is comparable in nematic and lamellar (or smectic) phases if the elastic modulii K and K_1 in the two phases are similar. This is usually the case in thermotropic [22] as well as in lyotropic [5,63] liquid crystals, the typical range being 1–10 pN.

Figure 4 shows the transverse orientational correlation function $H_\perp(r_\perp)$, calculated numerically from Eqs. (4.6) and (4.7) with the lower integration limit $q_\perp=\pi/L_\perp$ extended to $q_\perp=0$ (permissible if $\xi_B \ll L_\perp$). Although clearly not exponential, $H_\perp(r_\perp)$ has essentially decayed to zero at $r_\perp=\xi_K$, justifying the interpretation of ξ_K as a transverse orientational correlation length [26]. However, $H_\perp(r_\perp)$ does not approach zero monotonically, but first passes through a negative region with anticorrelated membrane normals, shown on a magnified scale in Fig. 5. This coherent feature is a signature of coupled membranes, not present for a free membrane. [When examining the large-$r_\perp$ behavior of $H_\perp(r_\perp)$ in Eq. (4.10), we must, of course, ensure that $L_\perp > r_\perp$.]

The physical significance of the different regimes in the decay of $H_\perp(r_\perp)$ is as follows. On transverse length scales up to $r_\perp \approx \xi_K$, the loss of orientational correlation in a given membrane is affected only by interactions with the two adjacent membranes. In this regime, the behavior of $H_\perp(r_\perp)$ is essentially the same as for a fluid membrane confined between two rigid plates [26]. The large initial decay of $H_\perp(r_\perp)$ (cf. Fig. 4), as well as the first negative peak (cf. Fig. 5), are therefore independent of the number N of membranes in the stack. In the region of the negative peak, where $r_\perp$ is still of order ξ_K, $\mathbf{n}_\perp(0)$ and $\mathbf{n}_\perp(r_\perp)$ have a slight preference for anti-parallel orientation. This is, indeed, the expected behavior after the first ''collision'' between adjacent membranes, where the ''wandering'' membranes change direction.

On transverse length scales between ξ_K and ξ_B, the interacting membranes exhibit coherent fluctuations (cf. Fig. 3), giving rise to the N-dependent negative feature in $H_\perp(r_\perp)$ (cf. Fig. 5). This regime terminates at $r_\perp \approx \xi_B$, because modes of longer wavelengths are essentially compressional, and, hence, cannot affect membrane orientation. The description of orientational correlations in a lamellar stack of membranes thus involves two distinct length scales: ξ_K and ξ_B, related to the loss of orientational correlations associated with incoherent short-wavelength modes (ξ_K) and coherent long-wavelength modes (ξ_B). This is perhaps seen more directly in the transverse orientational structure factor

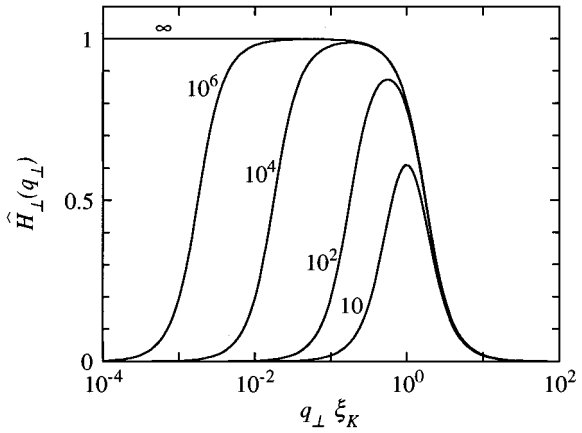

FIG. 6. Transverse orientational structure factor, $\hat{H}_\perp(q_\perp)$, for a stack of N (as indicated) coupled membranes, calculated from Eq. (4.7). The ordinate is in units of $k_BT\xi_K^2/(2A\kappa)$.

$\hat{H}_\perp(q_\perp)$, which governs the mean amplitude of transverse orientational modes (cf. Fig. 6). Since $\hat{H}_\perp(0)=0$ (for finite N), it follows that the integral of $H_\perp(r_\perp)$ over the base plane must vanish. Although not directly evident in the semilog plot of Fig. 5, the integrals over $H_\perp(r_\perp)$ are independent of N and equal in magnitude to the integral over the (N-independent) positive part of $H_\perp(r_\perp)$ in Fig. 4.

V. MAGNETIC-FIELD EFFECTS

A. Magnetic coherence length

As a consequence of the anisotropy of the molecular diamagnetic susceptibility tensor, an external magnetic field exerts a significant torque on a sufficiently large part of any system possessing long-range orientational order. In the presence of a magnetic field, the elastic free-energy functional (3.1) of a lamellar phase must be supplemented with a magnetic term [34,64]

$$\mathcal{F}_M[u(\mathbf{r})] = -\tfrac{1}{2}\int d\mathbf{r}(4\pi/\mu_0)\Delta\chi[\mathbf{B}_0\cdot\mathbf{n}(\mathbf{r})]^2$$
$$= \tfrac{1}{2}(4\pi/\mu_0)\Delta\chi B_0^2\int d\mathbf{r}$$
$$\times\left[\cos(2\beta)\left(\frac{\partial u}{\partial x}\right)^2+\cos^2\beta\left(\frac{\partial u}{\partial y}\right)^2\right], \quad (5.1)$$

where μ_0 is the vacuum permeability, $\Delta\chi=\chi_z-\chi_\perp$ the macroscopic diamagnetic susceptibility anisotropy, and $\mathbf{B_0}$ the uniform external magnetic field. (We use SI units throughout.) To obtain the second form in Eq. (5.1), we have invoked the harmonic approximation (2.9) and introduced the angle β (cf. Fig. 1) between the optic axis (z) and the magnetic field (which, by convention, is in the x-z plane [34]).

Fourier expanding the displacement field $u(\mathbf{r})$ in Eq. (5.1) and applying the equipartition theorem to $\mathcal{F}[\{\hat{u}(\mathbf{q})\}]+\mathcal{F}_M[\{\hat{u}(\mathbf{q})\}]$, we obtain, for the orientational structure factor in the presence of a magnetic field,

$$\hat{H}(\mathbf{q}) = \frac{k_BT}{V}\frac{q_\perp^2}{K_1q_\perp^2[q_\perp^2+\xi_M^{-2}f(\varphi;\beta)]+\overline{B}q_z^2}, \quad (5.2)$$

where we introduced the angular function

$$f(\varphi;\beta) = \mathrm{sgn}(\Delta\chi)[\cos^2\varphi\,\cos(2\beta)+\sin^2\varphi\,\cos^2\beta], \quad (5.3)$$

with φ the angle between the x axis and the $\mathbf{q}$ vector. Further, ξ_M is the magnetic coherence length [44], defined as

$$\xi_M = \left(\frac{\mu_0}{4\pi}\frac{K_1}{|\Delta\chi|}\right)^{1/2}\frac{1}{B_0}. \quad (5.4)$$

The physical significance of the magnetic coherence length is as follows: for a spatial region of linear dimension of order ξ_M or larger, the net magnetic torque is stronger than the elastic torque that maintains the macroscopic orientation induced by the boundary conditions, and, hence, the optic axis of that region tends to reorient so as to minimize the magnetic energy. This behavior is well known for nematic phases, which are readily aligned by moderately strong magnetic fields [22].

B. Magnetic-field effect on a free membrane

In the absence of membrane coupling, a lamellar phase would respond to a magnetic field in much the same way as a nematic phase. For example, a magnetic field along the optic axis ($\beta=0$) of a diamagnetically positive ($\Delta\chi>0$) lamellar phase strongly suppresses director fluctuation modes of wavelengths longer than the magnetic coherence length. Inserting Eq. (5.2) with $\overline{B}=0$ into Eq. (4.5), and assuming that $L_z \gg d$, we obtain, for $a \ll r_\perp \ll L_\perp$,

$$H_\perp(r_\perp) = \frac{k_BT}{2\pi\kappa}K_0(r_\perp/\xi_M), \quad (5.5)$$

and, for $a \ll \xi_M \ll L_\perp$,

$$\langle n_\perp^2\rangle = \frac{k_BT}{2\pi\kappa}\ln(\pi\xi_M/a). \quad (5.6)$$

A comparison of Eqs. (5.6) and (4.11) shows that, in the presence of a magnetic field (which might be the geomagnetic field), even a free membrane possesses true long-range orientational order. The modified Bessel function in Eq. (5.5) goes as $\ln(\xi_M/r_\perp)$ for $r_\perp \ll \xi_M$ and as $(\pi\xi_M/2r_\perp)^{1/2}\exp(-r_\perp/\xi_M)$ for $r_\perp \gg \xi_M$. On length scales much shorter than the magnetic coherence length, the orientational correlation thus decays logarithmically as in the field-free case, Eq. (4.10), whereas, on length scales much longer than ξ_M, $H_\perp(r_\perp)$ exhibits an essentially exponential decay with ξ_M playing the role of a transverse orientational correlation length, in close analogy with the (three-dimensional) nematic case [22].

C. Magnetic-field effect on coupled membranes

A lamellar phase differs fundamentally from a nematic phase in that it possesses (quasi) long-range positional order in one dimension. In the absence of defects, the repulsion

between adjacent membranes (or, at least, their excluded volume) strongly opposes the magnetic torque, which, in the absence of membrane coupling, would tend to realign the optic axis. In fact, under most conditions the magnetic-field effect can be neglected for lamellar phases. To show this, we rewrite the orientational structure factor in Eq. (5.2) as

$$\hat{H}(\mathbf{q}) = \frac{k_B T \xi_K^2}{V K_1} \frac{x}{x^2 + (\xi_K/\xi_M)^2 f(\varphi;\beta) x + (q_z d)^2}. \tag{5.7}$$

Since the denominator is a quadratic polynomial in $x = (q_\perp \xi_K)^2$, it follows that the magnetic term (linear in x) can be neglected if, for all φ and q_z, $\frac{1}{2}(\xi_K/\xi_M)^2 |f(\varphi;\beta)| \ll |q_z d|$. Since $|f(\varphi;\beta)| \leq 1$ and $|q_z d| \leq \pi/N$, the magnetic-field effect on the orientational structure factor can therefore be neglected if

$$\xi_M \gg \xi_B/(2\pi)^{1/2}. \tag{5.8}$$

The physical basis of this condition is clear. Only distortion modes with transverse wavelengths in the range $\xi_M \ll 1/q_\perp \ll \xi_B$ can be magnetically influenced; at shorter wavelengths the magnetic torque cannot compete with the elastic torque, at longer wavelengths the modes do not affect membrane orientation. If inequality (5.8) is satisfied, such a range does not exist. In terms of the magnetic-field strength B_0, condition (5.8) reads

$$B_0^2 \ll \frac{\mu_0 [\kappa w''(d)]^{1/2}}{2 \Delta\chi L_z}. \tag{5.9}$$

D. Broken symmetry

When condition (5.8) is violated, we must recognize that an external magnetic field generally breaks the intrinsic uniaxial symmetry of a lamellar phase. As is evident from the unsymmetrical dependence on x and y in Eq. (5.1), this is the case whenever the magnetic field and the optic axis are not collinear ($\beta \neq 0$). As a consequence of the broken symmetry, the orientation dependence of the lab-frame spectral densities is no longer given by Eq. (2.3). In fact, there are now five, rather than three, distinct irreducible crystal-frame spectral densities [34,36]. In the harmonic regime, however, director fluctuations still contribute only a single term to the secular lab-frame spectral density, as in Eq. (2.6), but the time correlation function is now [34]

$$G(\tau) = 3\langle n_x(0) n_x(\tau)\rangle - \langle n_y(0) n_y(\tau)\rangle, \tag{5.10}$$

which reduces to Eq. (2.8) in the field-free case. Equation (2.14) must therefore be generalized to

$$G(\tau) = \sum_{\mathbf{q}} (4\cos^2\varphi - 1) \hat{H}(\mathbf{q}) F(\mathbf{q},\tau). \tag{5.11}$$

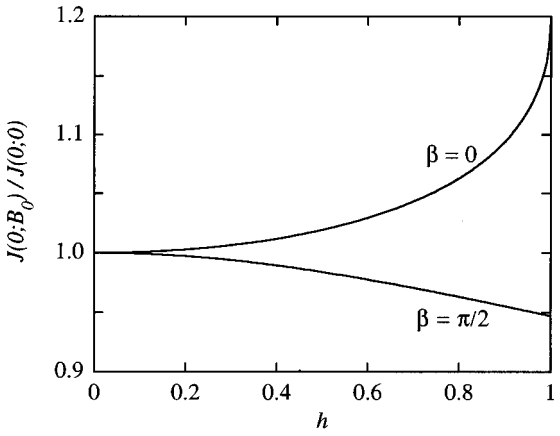

FIG. 7. Magnetic-field effect on the adiabatic spectral density $J(0)$ in a lamellar phase with $\Delta\chi < 0$ and the field parallel ($\beta = 0$) or perpendicular ($\beta = \pi/2$) to the optic axis. $J(0)$ was calculated from Eq. (5.12) with $N = 10^4$.

Under conditions where $F(\mathbf{q},\tau) = \exp(-q_\perp^2 D_\perp \tau)$ (cf. Sec. VI), the relative magnetic-field effect on the adiabatic spectral density is obtained from Eqs. (5.2) and (5.11) as

$$\frac{J(0;B_0)}{J(0;0)} = \frac{4}{\pi^2 \ln N} \int_0^{\pi/2} d\varphi (4\cos^2\varphi - 1) \times \int_1^N d\upsilon \frac{\left[\frac{\pi}{2} - \arctan \frac{h^2 f}{(\upsilon^2 - h^4 f^2)^{1/2}}\right]}{(\upsilon^2 - h^4 f^2)^{1/2}}, \tag{5.12}$$

with f as defined in Eq. (5.3) and $h = \xi_B/(\xi_M \sqrt{2\pi})$ a field parameter proportional to B_0. Equation (5.12) holds for $h < 1$. Most lamellar phases have $\Delta\chi < 0$, so that the magnetic free energy is minimized with the optic axis perpendicular to the magnetic field. The configuration $\beta = \pi/2$ is thus stable, whereas $\beta = 0$ is metastable. As expected, we see in Fig. 7 that the magnetic field suppresses director fluctuations for $\beta = \pi/2$, whereas it enhances them for $\beta = 0$. It should be noted that, since the field effect depends on β, the lab-frame spectral density has an implicit orientation dependence, apart from the explicit one displayed in Eq. (2.3).

The divergence at $h = 1$ of the director fluctuations in the metastable configuration ($\beta = 0$ for $\Delta\chi < 0$ or $\beta = \pi/2$ for $\Delta\chi > 0$) signals a breakdown of the harmonic theory. At the critical magnetic field ($h = 1$), the lamellar phase undergoes a transition to a buckled phase where the ground-state configuration of the fluid membranes is no longer flat but exhibits a (static) periodic undulation of wavelength $(2\pi)^{1/2}\xi_B$ and amplitude of order ξ_K^2/d [64]. This buckling instability, or Helfrich-Hurault transition [22], results from the interplay of magnetic and elastic torques and boundary conditions. The stability condition $h < 1$, or $(2\pi)^{1/2}\xi_M > \xi_B$, may be compared with the analogous condition, $\pi\xi_M > L_z$, for stability with respect to the Fréedericksz transition in a nematic phase [22]. Since ξ_M is typically only one order of magnitude larger in nematic phases while $L_z \gg \xi_B$, it is clear that

magnetic-field effects are much more important in nematic phases than in lamellar phases.

VI. DYNAMICS OF ORIENTATIONAL FLUCTUATIONS IN A LAMELLAR PHASE

A. Diffusion on a fluctuating membrane

On the supermolecular length and time scales of interest here, the single-particle motion of the spin-bearing molecule obeys the classical diffusion equation. The single-particle correlation function in Eq. (2.17) can then be identified as the spatial Fourier transform of the Green's function for the diffusion equation, i.e.,

$$F_S(\mathbf{q},\tau)=\exp[-(q_\perp^2 D_\perp^S+q_z^2 D_z^S)\tau], \tag{6.1}$$

where $D_\perp^S$ and D_z^S are the self-diffusion coefficients for motion in the base plane and along the optic axis, respectively. We assume that diffusion across the membranes is negligibly slow, i.e., we set $D_z^S=0$. It can be shown that the effect of longitudinal diffusion on $J(0)$ can be neglected if

$$\frac{D_z^S}{D_\perp^S}\ll\frac{d^2}{4\xi_K^2}\frac{\ln N}{\ln(L_\perp/a)}. \tag{6.2}$$

This inequality may not be satisfied in thermotropic smectic-A phases [65], but should hold in lyotropic lamellar phases free from microscopic structural defects [66,67].

The transverse self-diffusion coefficient $D_\perp^S$ in Eq. (6.1) refers to projected displacements in the base plane. In general, $D_\perp^S$ is smaller than the curvilinear self-diffusion coefficient D_0 that characterizes molecular motion on the undulating membrane. If membrane undulation is much faster than diffusion (the limit of annealed disorder), the base-plane diffusion coefficient is [68]

$$D_\perp^S=(1-\tfrac{1}{2}\langle n_\perp^2\rangle)D_0. \tag{6.3}$$

In the opposite (more realistic) limit of slow undulations (quenched disorder), $D_\perp^S$ is in general smaller than in the annealed limit. Within the harmonic regime, however, the results for $D_\perp^S$ in the two limits coincide [68]. It appears, therefore, that the projected diffusion process is independent of the dynamics of membrane undulation, as long as the undulation amplitude is sufficiently small (harmonic regime), justifying the factorization of the total correlation function $F(\mathbf{q},\tau)$ in Eq. (2.22). Such a factorization is not possible for a strongly fluctuating membrane, as can be shown explicitly for one-dimensional models [69].

B. Hydrodynamic modes in a lamellar phase

In the general case, the hydrodynamics of a lamellar phase features seven coupled modes [22,70]. Nuclear spin relaxation, however, is only affected by low-frequency ($\ll$MHz) modes that modulate the membrane curvature. At the low frequencies of interest here, the system can be regarded as incompressible and athermal, whereby only three coupled modes have to be retained [23,71]. In the special case of a purely transverse wave vector ($\mathbf{q}=\mathbf{q}_\perp$), these include two high-frequency modes (transverse shear and membrane peristaltic), which can be disregarded, and a low-frequency undulation mode with a characteristic frequency [44]

$$\Gamma=\frac{\kappa}{\eta d}q_\perp^2, \tag{6.4}$$

where η is an effective shear viscosity. In the undulation mode, each membrane in the stack fluctuates independently from the others, unaffected by the direct membrane coupling $w(s)$. There is, however, a hydrodynamic coupling between adjacent membranes (at a mean distance d). This distinguishes the undulation mode from the single-membrane (Zimm) mode, $\Gamma=\kappa q_\perp^3/(4\eta)$, where only the hydrodynamic self-interaction is present [21]. In a lamellar phase, the single-membrane mode is relevant only for $q_\perp d\gg 1$ [72,73] and, like other high-frequency subhydrodynamic modes [74–76], is of no consequence for spin relaxation.

As expected, the direct membrane interaction comes into play for oblique wave vectors ($q_z\neq 0$). In this more general case, the dominant low-frequency mode, referred to as the baroclinic mode, has a dispersion relation of the form [23,77,78]

$$\Gamma=\frac{\kappa}{\eta d}q_\perp^2\frac{q_\perp^4+q_z^2d^2/\xi_K^4}{q^4+\alpha q_z^2/d^2}. \tag{6.5}$$

For $q_z=0$, this baroclinic mode degenerates into the pure undulation mode (6.4). For $q_\perp\xi_K\ll q_z d\ll 1$, it reduces to the so-called slip mode [23]

$$\Gamma=\frac{\kappa d^3}{\alpha\eta\xi_K^4}q_\perp^2=\frac{d^2}{\alpha\eta}\overline{B}q_\perp^2, \tag{6.6}$$

where Eq. (4.8) was used in the last step. In contrast to the undulation mode, the slip (and baroclinic) mode involves a lateral flow of the intermembrane fluid as the membrane separation is modulated. This gives rise to the α term in Eq. (6.5). Using a discrete-membrane-stack model of the lamellar phase, one obtains $\alpha=12$ when the membrane thickness is small compared to d [23,73].

Some remarks are in order regarding the microscopic interpretation of the phenomenological coefficients that appear in the hydrodynamic analysis. First, the effect of membrane stretching has been ignored. Although the membranes were taken to be locally incompressible, a corrugated membrane has a finite lateral compressibility [79], which leads to a slight slowing down of the modes [77,80]. Second, membrane corrugation on short wavelengths also reduces the bending rigidity, leading to a $q_\perp$-dependent logarithmic renormalization of κ [27,81]. For long wavelengths ($q_\perp\xi_K\ll 1$), the effective κ should thus be slightly smaller than the bare (short-wavelength) rigidity [5]. In principle, the mode relaxation rate Γ should also be renormalized. A recent study shows, however, that the single-membrane mode does not renormalize [79]. Third, most hydrodynamic treatments of stacked-membrane models have focused on dilute lamellar phases, where the membrane spacing d is large compared to the membrane thickness. If this is not the case, as in most phospholipid-water systems, the hydrodynamic (and equilibrium) parameters must be interpreted accordingly [23,71,82].

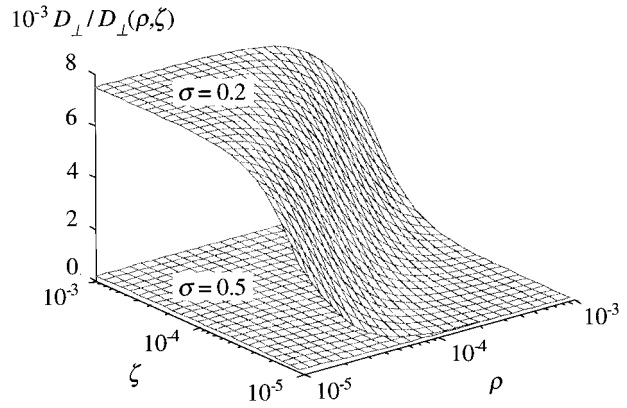

FIG. 8. Wave-vector dependence of the inverse of the effective transverse diffusion coefficient $D_\perp(\mathbf{q})$, calculated from Eq. (6.8), with $\delta=0$ (no molecular diffusion) and the indicated values of the coupling parameter σ.

According to the fluctuation-dissipation theorem, the characteristic mode frequency Γ emerging from a linearized hydrodynamic treatment can be identified with the inverse correlation time of the displacement-mode time correlation function in Eq. (2.18). By combining Eqs. (2.22), (6.1), and (6.5), we can thus express the total mode correlation function as

$$F(\mathbf{q},\tau)=\exp[-q_\perp^2 D_\perp(\mathbf{q})\tau], \tag{6.7}$$

with an apparent, wave-vector-dependent, transverse ''diffusion coefficient'' $D_\perp(\mathbf{q})$ given by

$$D_\perp(\mathbf{q})=D_\perp\left[\delta+(1-\delta)\,\frac{\sigma^4(\rho^2+\zeta^2)}{(\sigma^2\rho+\pi\zeta^2)^2+\alpha\zeta^2}\right], \tag{6.8}$$

with the reduced variables $\rho=(q_\perp\xi_K)^2/\pi$ and $\zeta=q_z d/\pi$. Further, we have introduced the relative diffusion coefficient

$$\delta=D_\perp^S/D_\perp\,, \tag{6.9}$$

with $D_\perp=D_\perp^S+D_\perp^C$ and $D_\perp^C=\kappa/(\eta d)$. Finally, we have defined the coupling parameter

$$\sigma=d/\xi_K\,. \tag{6.10}$$

For strongly coupled membranes, the patch length ξ_K is short and σ large, and vice versa.

If the membrane coupling is not too strong ($\sigma<1$), the baroclinic mode can be several orders of magnitude slower in the slip limit (where coupling is most strongly manifested) than in the undulation limit (cf. Fig. 8). At low frequencies, the spectral density function $J(\omega)$ in Eq. (2.23) will therefore be profoundly affected by membrane coupling, not only via the static orientational structure factor $\hat{H}(\mathbf{q})$, but also via the dynamic structure factor $S(\mathbf{q},\omega)$ resulting from Eqs. (2.24) and (6.7).

VII. TIME CORRELATION FUNCTION AND SPECTRAL DENSITY IN THE FAST-DIFFUSION LIMIT

We are now fully equipped to address the central issue of this work, the calculation of the orientational time correlation function $G(\tau)$ in Eq. (2.8) and the associated spectral density function $J(\omega)$. Unless otherwise noted, we assume that condition (5.8) is satisfied so that the magnetic-field effects discussed in Sec. V can be ignored. In this section, we consider the limiting case where molecular diffusion is much faster than collective membrane dynamics. We then have $D_\perp^S \gg D_\perp^C$, so that $\delta=1$ in Eq. (6.8) and

$$F(\mathbf{q},\tau)=\exp(-q_\perp^2 D_\perp^S\tau). \tag{7.1}$$

For the following development, it is convenient to introduce four characteristic frequencies. Two are associated with the transverse cutoffs

$$\omega_a=\pi^2 D_\perp^S/a^2, \tag{7.2}$$

$$\omega_L=\pi^2 D_\perp^S/L_\perp^2, \tag{7.3}$$

and two are related to the orientational correlation lengths

$$\omega_K^S=\pi D_\perp^S/\xi_K^2, \tag{7.4}$$

$$\omega_B=\pi D_\perp^S/\xi_B^2. \tag{7.5}$$

From Eqs. (4.8) and (4.9) it follows that $\omega_B=\omega_K^S/N$, i.e., these frequencies typically differ by four orders magnitude or more.

A. Time correlation function

Inserting Eq. (7.1) into Eq. (2.21), converting the sum over $\mathbf{q}$ to an integral over $(q_\perp,\varphi,q_z)$, and making use of Eq. (4.5), we obtain

$$G(\tau)=\frac{A}{2\pi}\int dq_\perp q_\perp \hat{H}_\perp(q_\perp)\exp(-q_\perp^2 D_\perp^S\tau). \tag{7.6}$$

As seen from Fig. 6, $\hat{H}_\perp(q_\perp)$ goes to zero for $q_\perp \ll 1/\xi_B$. As long as $\xi_B \ll L_\perp$, we can therefore extend the lower integration limit in Eq. (7.6) from $\pi/L_\perp$ to 0, making $G(\tau)$ independent of membrane size ($L_\perp$). This is a direct consequence of membrane coupling, which makes the orientational correlation function $H_\perp(r_\perp)$ vanish for $r_\perp>\xi_B$ (cf. Fig. 5). In contrast, for a free membrane, $H_\perp(r_\perp)$ decays only logarithmically [cf. Eq. (4.10)], whereby $G(\tau)$ depends on $L_\perp$ at all times. In particular, $G(0)\propto \ln L_\perp$ [cf. Eq. (4.11)] and $J(0)\propto L_\perp^2$ [6]. For a free membrane, however, the magnetic-field effect on $\hat{H}_\perp(q_\perp)$ cannot be ignored and this will reduce, but not eliminate, the dependence of $G(\tau)$ on membrane size [6].

We are only interested in the behavior of $G(\tau)$ on time scales $\tau \gg 1/\omega_a$, where diffusion-induced director fluctuations are slower than local molecular motions. Provided that $\xi_K \gg a$, we can then extend the upper integration limit in Eq. (7.6) from π/a to ∞. Inserting $\hat{H}_\perp(q_\perp)$ from Eq. (4.7) into Eq. (7.6), and integrating over $q_\perp$ (from 0 to ∞), we find

$$G(\tau)=\frac{k_B T}{4\pi\kappa}\,\frac{1}{\omega_K^S\tau}\,[g(\omega_B\tau)-g(\omega_K^S\tau)], \tag{7.7}$$

with the auxiliary function $g(x)$ defined in terms of the sine and cosine integrals as

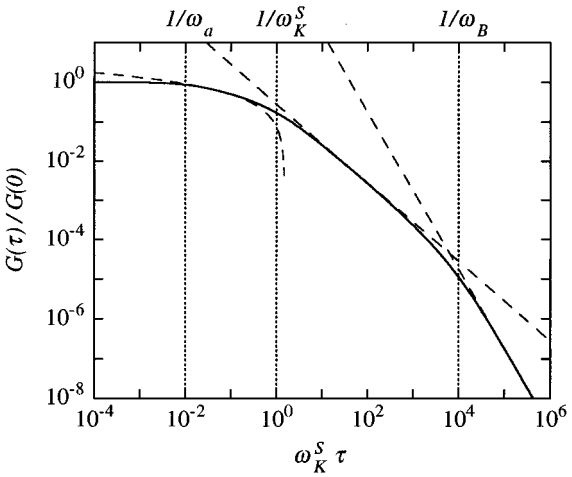

FIG. 9. Decay of the time correlation function $G(\tau)$ in the fast-diffusion limit. The solid curve was obtained by numerical integration of Eq. (7.6) over the range $0 \leqslant q_\perp \leqslant \pi/a$. On this scale, it is indistinguishable from the analytical result in Eq. (7.7). The dashed curves correspond to the limiting results. Eqs. (7.9)–(7.11). The parameter values are $N=10^4$ and $\pi(\xi_K/a)^2=100$.

$$g(x)=\mathrm{Ci}(x)\sin x-[\mathrm{Si}(x)-\pi/2]\cos x. \tag{7.8}$$

Using the appropriate expansions of the auxiliary function $g(x)$ [83], we can identify three distinct regimes in the decay of $G(\tau)$. In the short-time regime, $1/\omega_a \ll \tau \ll 1/\omega_K^S$, Eq. (7.7) reduces to

$$G(\tau)=\frac{k_BT}{4\pi\kappa}\,[1-\gamma-\ln(\omega_K^S\tau)], \tag{7.9}$$

where $\gamma=0.5772\ldots$ is Euler's constant. In this regime, the molecule has not yet diffused out of the initial membrane patch of area ξ_K^2, and $G(\tau)$ is nearly the same as for a free membrane of size $L_\perp=\xi_K$.

In the intermediate-time regime, $1/\omega_K^S \ll \tau \ll 1/\omega_B$, Eq. (7.7) yields

$$G(\tau)=\frac{k_BT}{8\kappa\omega_K^S\tau}, \tag{7.10}$$

and in the long-time regime, $\tau \gg 1/\omega_B$,

$$G(\tau)=\frac{k_BT}{4\pi\kappa\omega_K^S\omega_B\tau^2}. \tag{7.11}$$

Membrane coupling is strongly manifested in both these regimes, $G(\tau)$ being proportional to ξ_K^2 or $\xi_K^2\xi_B^2$, respectively. Figure 9 shows the decay of $G(\tau)$, illustrating the accuracy of Eqs. (7.9)–(7.11) in their respective regimes.

B. Asymptotic behavior of $G(\tau)$

The asymptotic decay in Eq. (7.11), $G(\tau)\sim\tau^{-2}$, is somewhat counterintuitive, since time correlation functions involving translational diffusion in D unbounded dimensions generally have the same asymptotic form as the diffusion propagator, i.e., $G(\tau)\sim\tau^{-D/2}$. This is the case for orientational fluctuations due to one-dimensional diffusion along a semiflexible space curve [84,85], or three-dimensional diffusion in a nematic phase in the presence of a magnetic field [85,86], as well as for modulation of the internuclear vector by relative translational diffusion in two-dimensional systems [30–32].

To identify the physical basis for the unexpected asymptotic behavior of $G(\tau)$, we return to Eq. (7.6). We note that, for large τ, only small $q_\perp$ values contribute to the integral. Taylor expanding $\hat{H}_\perp(q_\perp)$ around $q_\perp=0$ and performing the resulting standard $q_\perp$ integrals, we obtain

$$G(\tau)=\frac{A}{4\pi}\left[\hat{H}_\perp(0)(D_\perp^S\tau)^{-1}+\frac{\sqrt{\pi}}{2}\,\hat{H}_\perp'(0)(D_\perp^S\tau)^{-3/2}\right.$$
$$\left.+\tfrac{1}{2}\hat{H}_\perp''(0)(D_\perp^S\tau)^{-2}+\cdots\right], \tag{7.12}$$

where a prime signifies differentiation with respect to $q_\perp$. From Eq. (4.7), we obtain $\hat{H}_\perp(0)=0$, $\hat{H}_\perp'(0)=0$, and $\hat{H}_\perp''(0)=2k_BT\xi_K^2\xi_B^2/(\pi^2A\kappa)$, which, when inserted into Eq. (7.12), reproduces the long-time limit, Eq. (7.11). To obtain $G(\tau)\sim\tau^{-1}$, we must clearly have $\hat{H}_\perp(0)\neq 0$, which would be the case for an exponentially decaying orientational correlation function $H_\perp(r_\perp)$. We can conclude, therefore, that the faster asymptotic decay of $G(\tau)$ is a consequence of the anticorrelation of membrane normals in the range $\xi_K<r_\perp<\xi_B$ (cf. Fig. 5), induced by coherent undulations of many coupled membranes in a multilamellar stack (cf. Sec. IV D).

It is interesting to note that the asymptotic $G(\tau)\sim\tau^{-2}$ decay in Eq. (7.11) applies only to a lamellar stack with a finite number of membranes. In the limit $N\to\infty$, also $\xi_B\to\infty$, so the regime $\tau\gg 1/\omega_B$ does not exist. The asymptotic behavior is now given by Eq. (7.10), i.e., we have $G(\tau)\sim\tau^{-1}$. This result also emerges from Eq. (7.12), since, for $N\to\infty$, Eq. (4.7) yields

$$\hat{H}_\perp(0)=\frac{k_BT}{A}\,\frac{\xi_K^2}{2\kappa}. \tag{7.13}$$

According to the fluctuation-dissipation theorem [1], the quantity $\xi_K^2/(2\kappa)$ may be interpreted as an orientational susceptibility, which is nonzero only in the limit $N\to\infty$. The slower asymptotic decay of $G(\tau)$ for an infinite stack of membranes, and the consequent logarithmic divergence of $J(0)$, are manifestations of the well-known Landau-Peierls instability: for any three-dimensional system exhibiting one-dimensional periodicity, thermal fluctuations destroy the long-range order in the thermodynamic limit [1]. Although theoretically illuminating, these considerations are of little practical concern. First, real systems are finite. Second, in the presence of an external magnetic field (which could be the NMR field or the geomagnetic field), condition (5.8) will ultimately be violated as N increases. When this happens, the magnetic coherence length ξ_M replaces ξ_B as the transverse cutoff, again making $\hat{H}_\perp(0)=0$. Now, however, we have $\hat{H}_\perp'(0)\neq 0$, leading, with Eq. (7.12), to

$$G(\tau)\sim\frac{k_BT}{16\kappa\omega_K^S\omega_M^{1/2}\tau^{3/2}}, \tag{7.14}$$

with $\omega_M = \pi D_\perp^S / \xi_M^2$. This result pertains to the stable configuration with $\beta = 0$ and $\Delta\chi > 0$. Third, on sufficiently long time scales, longitudinal diffusion cannot be ignored ($D_z^S \neq 0$); this would again lead to $G(\tau) \sim \tau^{-3/2}$. Fourth, if the membranes are laterally bounded (finite $L_\perp$), all terms in Eq. (7.12) include exponential factors and $G(\tau) \sim \exp(-\omega_L \tau)/\tau$. For a typical sample, however, $\xi_B \ll \xi_M, L_\perp$ and then the Landau-Peierls instability and the effects of magnetic field, longitudinal diffusion, and finite membrane dimensions can all be neglected.

C. Spectral density function

The spectral density function is obtained from Eqs. (2.7) and (7.6) as

$$J(\omega) = \frac{A}{2\pi D_\perp^S} \int dq_\perp \, \frac{q_\perp^3 \hat{H}_\perp(q_\perp)}{q_\perp^4 + (\omega/D_\perp^S)^2}. \tag{7.15}$$

Substituting $\hat{H}_\perp(q_\perp)$ from Eq. (4.7) and integrating over $q_\perp$ from 0 to ∞, which is permissible when $\xi_K \gg a$, $\xi_B \ll L_\perp$, and $\omega \ll \omega_a$, we obtain the surprisingly simple result [6,39]

$$J(\omega) = \frac{k_B T}{8\kappa\omega_K^S} \ln\left(\frac{\omega + \omega_K^S}{\omega + \omega_B}\right). \tag{7.16}$$

If the restriction $\omega \ll \omega_a$ is removed, the ln term is supplemented with a term $(2/\pi)(\omega_K^S/\omega)\arctan(\omega_a/\omega)$, yielding a high-frequency dispersion step that is always negligible compared to that produced by local molecular motions. At lower frequencies, $\omega \ll \omega_a$, the arctan term adds a constant contribution to $J(\omega)$ that is generally (when $\xi_K \gg a$) negligible compared to that coming from the ln term.

The adiabatic limit of Eq. (7.16) is

$$J(0) = \frac{k_B T}{8\kappa\omega_K^S} \ln N. \tag{7.17}$$

As noted in Sec. VII B, the logarithmic divergence of $J(0)$ as $N \to \infty$ is a manifestation of the Landau-Peierls instability [1]. This connection is made more explicit by noting that

$$J(0) = \langle u^2 \rangle / D_\perp^S, \tag{7.18}$$

which follows by combining Eqs. (2.7), (2.19), (2.21), and (7.1). This peculiar result, relating the adiabatic spectral density associated with the time correlation function (2.8) for membrane orientation to the mean square fluctuation in membrane position, is simply a consequence of canceling $q_\perp^2$ factors from Eqs. (2.19) and (7.1), each originating from two transverse space derivatives.

Like most other results in this section, Eq. (7.17) assumes that condition (5.8) is satisfied. In the presence of a magnetic field, however weak, condition (5.8) is violated for sufficiently large N. When the magnetic field is taken into account, $J(0)$ no longer diverges for $N \to \infty$. For $\beta = 0$ and $\Delta\chi > 0$, we obtain

$$J(0) = \frac{k_B T \xi_K^2}{4\pi\kappa} \ln(2\pi^{1/2}\xi_M/\xi_K), \tag{7.19}$$

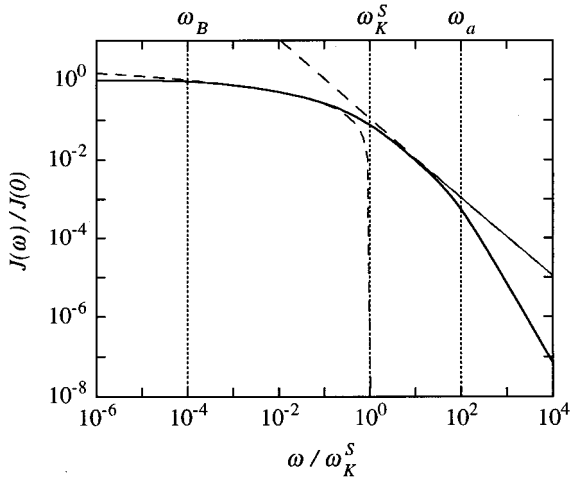

FIG. 10. Dispersion of the spectral density function $J(\omega)$ in the fast-diffusion limit. The thick solid curve was obtained by numerical integration of Eq. (7.15) over the range $0 \leq q_\perp \leq \pi/a$, and the thin solid curve is the analytical result in Eq. (7.16). The dashed curves correspond to the limiting results, Eqs. (7.20) and (7.22). The parameter values are $N = 10^4$ and $\pi(\xi_K/a)^2 = 100$.

provided that $\xi_K \ll \xi_M \ll L_\perp, L_z$.

By expanding the logarithm in Eq. (7.16), we can identify three distinct frequency regimes in the dispersion of $J(\omega)$, analogous to the three time regimes in the decay of $G(\tau)$. In the low-frequency regime, $\omega \ll \omega_B$, we have simply $J(\omega) \approx J(0)$. In the intermediate-frequency regime, $\omega_B \ll \omega \ll \omega_K^S$, Eq. (7.16) reduces to

$$J(\omega) = \frac{k_B T}{8\kappa\omega_K^S} \ln(\omega_K^S/\omega). \tag{7.20}$$

As expected, membrane coupling is manifested at all frequencies below the diffusional patch frequency ω_K^S. At these frequencies, $J(\omega)$ is dominated by the $1/\tau$ decay of $G(\tau)$ on the intermediate timescale $1/\omega_K^S \ll \tau \ll 1/\omega_B$. Indeed, the adiabatic spectral density can be expressed as

$$J(0) = \int_{1/\omega_K^S}^{1/\omega_B} d\tau \, G(\tau), \tag{7.21}$$

which, after substitution of $G(\tau)$ from Eq. (7.10), leads to Eq. (7.17).

At frequencies exceeding the patch frequency, $\omega_K^S \ll \omega \ll \omega_a$, Eq. (7.16) reduces to the same form as for a free membrane,

$$J(\omega) = \frac{k_B T}{8\kappa\omega}. \tag{7.22}$$

Indeed, if the compressional term in Eq. (3.1) is omitted, one obtains, for $\omega \ll \omega_a$ [6],

$$J(\omega) = \frac{k_B T}{4\pi\kappa\omega} \arctan(\omega/\omega_L). \tag{7.23}$$

For $\omega \gg \omega_L$, this reduces to Eq. (7.22), as first shown by Marqusee, Warner, and Dill [19].

Figure 10 shows the full dispersion of $J(\omega)$, illustrating the accuracy of Eqs. (7.20) and (7.22) in their respective regimes. On an absolute scale, not normalized by $J(0)$, $J(\omega)$ is the same for coupled and free membranes at high frequencies, $\omega \gg \omega_K^S$. At lower frequencies, however, $J(\omega)$ becomes much larger for the free membrane. For the typical parameter values $N=10^4$ and $L_\perp/\xi_K=10^6$, the adiabatic spectral density $J(0)$ is some ten orders of magnitude larger for a free membrane than for a coupled membrane in a multilamellar stack.

The $1/\omega$ dispersion law in Eq. (7.22) is a truly remarkable result. It tells us that, in the high-frequency regime, the spin relaxation rate (proportional to $J(\omega)$) is entirely independent of the rate of orientational fluctuations. This counterintuitive result may be understood by noting that the diffusion coefficient $D_\perp^S$ enters via the mode correlation function as $\exp(-q_\perp^2 D_\perp^S \tau)$. Any dependence of $G(\tau)$ or $J(\omega)$ on $D_\perp^S$ must therefore appear in the form of one or more characteristic frequencies $\propto D_\perp^S/\xi^2$, with ξ one of the five correlation or cutoff lengths that characterize the transverse elastic modes of a lamellar phase: $L_\perp$, ξ_M, ξ_B, ξ_K, and a (usually decreasing in that order). A free membrane, however, possesses no intrinsic characteristic length, apart from the cutoff lengths a and $L_\perp$. As a result of this peculiar property of a free membrane, $J(\omega)$ must be independent of $D_\perp^S$ in the frequency range $\omega_L \ll \omega \ll \omega_a$. In the presence of a magnetic field, however, the magnetic coherence length ξ_M introduces the magnetic frequency $\omega_M=\pi D_\perp^S/\xi_M^2$, and Eq. (7.22) is replaced by (for $\beta=0$ and $\Delta\chi>0$)

$$J(\omega)=\frac{k_BT}{8\kappa\omega}\,\frac{1+\left(\frac{\omega_M}{\pi\omega}\right)\ln\left(\frac{\omega_M}{\pi\omega}\right)}{1+\left(\frac{\omega_M}{\pi\omega}\right)^2}. \tag{7.24}$$

For $\omega_M \ll \omega \ll \omega_a$, we recover Eq. (7.22), whereas, for $\omega_L \ll \omega \ll \omega_M$,

$$J(\omega)=\frac{k_BT}{4\kappa\omega_M}\ln\left(\frac{\omega_M}{\pi\omega}\right). \tag{7.25}$$

VIII. TIME CORRELATION FUNCTION AND SPECTRAL DENSITY FOR DIFFUSION AND COUPLED MEMBRANE UNDULATIONS

The results of Sec. VII are strictly valid only in the fast-diffusion limit, where $D_\perp^S \gg D_\perp^C$. When the observed nuclear spin resides in a large molecule, such as a phospholipid, director fluctuations are due mainly to collective membrane undulation, and the slow-diffusion limit ($D_\perp^S \ll D_\perp^C$) is more appropriate. In the following, we consider the general case, without any restrictions on the relative magnitudes of $D_\perp^S$ and $D_\perp^C$. The mode correlation function is then given by Eq. (6.7), with the wave-vector-dependent ''diffusion coefficient'' $D_\perp(\mathbf{q})$ in Eq. (6.8).

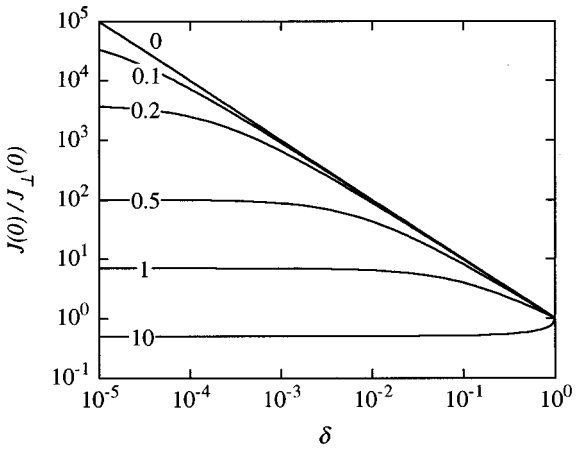

FIG. 11. The adiabatic spectral density $J(0)$, calculated from Eq. (8.2), relative to the fictitious spectral density $J_\perp(0)$, due solely to transverse modes. The parameter $\delta=D_\perp^S/(D_\perp^S+D_\perp^C)$ is varied at fixed $D_\perp^S+D_\perp^C$. The other parameter values are $N=10^4$, $\alpha=12$, and σ as indicated.

A. Adiabatic spectral density

In place of Eq. (7.18), we now have

$$J(0)=\sum_{\mathbf{q}}\frac{\langle|\hat{u}(\mathbf{q})|^2\rangle}{D_\perp(\mathbf{q})}. \tag{8.1}$$

Substituting $\langle|\hat{u}(\mathbf{q})|^2\rangle=\hat{H}(\mathbf{q})/q_\perp^2$ from Eq. (4.2) and $D_\perp(\mathbf{q})$ from Eq. (6.8) and integrating over $\mathbf{q}$ space, we obtain, for $\xi_K \gg a$ and $\xi_B \ll L_\perp$ (so that the $q_\perp$ limits can be set to 0 and ∞),

$$J(0)=\frac{k_BT}{8\kappa\omega_K\delta}\left\{\ln N-\frac{2}{\pi}(1-\delta)\sigma^2\times\int_{1/N}^1 d\zeta\,\frac{\arctan[\Delta/(\pi\delta\zeta)]}{\Delta\zeta}\right\}, \tag{8.2}$$

with $\omega_K=\pi(D_\perp^S+D_\perp^C)/\xi_K^2$ and

$$\Delta=[\delta\alpha+(1-\delta)(\sigma^4+\delta\pi^2\zeta^2)]^{1/2}. \tag{8.3}$$

The remaining parameters in Eq. (8.2) were defined in connection with Eq. (6.8). In the fast-diffusion limit ($D_\perp^S \gg D_\perp^C$), Eq. (8.2) reduces to Eq. (7.17), i.e.,

$$J(0)=\frac{k_BT\xi_K^2}{8\pi\kappa D_\perp^S}\ln N. \tag{8.4}$$

In the slow-diffusion limit ($D_\perp^S \ll D_\perp^C$), Eq. (8.2) yields

$$J(0)=\frac{k_BT\xi_K^6}{8\pi\kappa d^4 D_\perp^C}\left[\frac{\pi^2}{4}+2\sigma^2+\tfrac{1}{2}(\alpha+\sigma^4)\ln N\right]. \tag{8.5}$$

Figure 11 reveals a dramatic effect on the adiabatic spectral density $J(0)$ of dynamic membrane coupling via the oblique ($q_z\neq 0$) baroclinic distortion modes. The diffusivity ratio δ is varied here, but the sum $D_\perp^S+D_\perp^C$ is kept constant. We compare $J(0)$, calculated from Eq. (8.2), with a fictitious

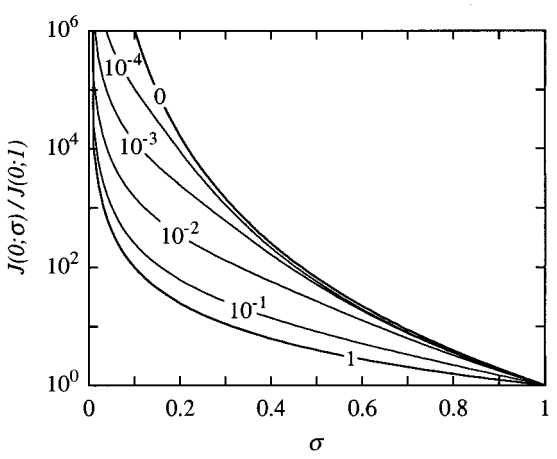

FIG. 12. Variation of the adiabatic spectral density $J(0)$, calculated from Eq. (8.2), with the membrane coupling parameter $\sigma = d/\xi_K$. The parameter values are $N=10^4$, $\alpha=12$, and δ as indicated.

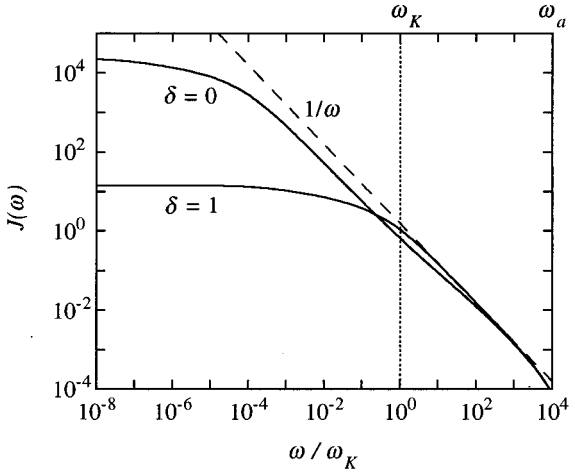

FIG. 13. Dispersion of the spectral density function $J(\omega)$, calculated from Eq. (8.6) with $\alpha=12$, $\sigma=0.25$, $N=10^4$, $\pi(\xi_K/a)^2 = 10^4$, and δ as indicated. The plotted $J(\omega)$ has been reduced by $k_BT/(4\pi\kappa\omega_K)$. The dashed line corresponds to the $1/\omega$ dispersion in Eq. (7.22).

spectral density $J_\perp(0)$, corresponding to purely transverse modes and thus given by Eq. (8.4) with $D_\perp^S$ replaced by $D_\perp^S + D_\perp^C$.

If membrane coupling is weak ($\sigma \ll 1$), the oblique baroclinic modes, being affected only by hydrodynamic interactions, are very slow (cf. Fig. 8). In this weak-coupling regime, collective membrane fluctuations can have an enormous effect on $J(0)$, but this effect is independent of the rate of the membrane fluctuations. In fact, for sufficiently small σ, $J(0)$ is given by Eq. (8.4), with no reference to $D_\perp^C$ (cf. the uppermost curve in Fig. 11). [Note that the limit $\sigma=0$ cannot be taken without violating the condition $\xi_B \ll L_\perp$, used in deriving Eq. (8.2), which requires that $\sigma \gg \sqrt{dL_z}/L_\perp$.] This somewhat paradoxical result can be understood by examining Eq. (6.8): when membrane coupling is weak ($\sigma \ll 1$), molecular diffusion can dominate $D_\perp$ even though $D_\perp^S \ll D_\perp^C$. The dynamics of weakly coupled membranes are simply not characterized by the ''diffusion coefficient'' $D_\perp^C$ for the much faster, purely transverse, undulation mode.

If membrane coupling is strong ($\sigma \gg 1$), the baroclinic modes are of small amplitude and decay rapidly (cf. lattice vibrations in a solid), competing efficiently with molecular diffusion. In this strong-coupling regime, the oblique baroclinic modes reduce $J(0)$ by a factor $(1-\sqrt{1-\delta})/\delta$ as compared to the purely transverse $J_\perp(0)$. When $D_\perp^S \ll D_\perp^C$, $J(0)$ is thus one-half of Eq. (8.4), with $D_\perp^S$ replaced by $D_\perp^C$ (cf. the lowermost curve in Fig. 11). (Note that the limit $\sigma \to \infty$ cannot be taken without violating the condition $\xi_K \gg a$, used in deriving Eq. (8.2), which requires that $\sigma \ll d/a$.)

Figure 12 displays the strong dependence of $J(0)$ on membrane coupling (both static and dynamic effects). The coupling parameter $\sigma = d/\xi_K$ is varied, while $D_\perp^S$ and $D_\perp^C$ are fixed. In the fast-diffusion limit ($\delta=1$), the static coupling effect makes $J(0) \sim \xi_K^2$, as predicted by Eq. (8.4). In the slow-diffusion limit ($\delta=0$), the dynamic coupling effect is also manifested, leading to $J(0) \sim \xi_K^6$, as predicted by Eq. (8.5) for $\sigma < 1$.

B. Spectral density dispersion

To calculate the spectral density function $J(\omega)$ in the general case, we start from Eq. (2.23), inserting the static structure factor $\hat{H}(\mathbf{q})$ from Eq. (4.2) and the (normalized) dynamic structure factor $S(\mathbf{q},\omega)$ from Eqs. (2.24) and (6.7). Converting the sum in Eq. (2.23) to an integral and introducing reduced variables as in Eq. (6.8), we obtain

$$J(\omega) = \frac{k_BT}{4\pi\kappa} \int d\rho \int d\zeta \, \frac{\rho}{(\rho^2+\zeta^2)} \, \frac{\rho\Omega_K(\rho,\zeta)}{[\rho^2\Omega_K^2(\rho,\zeta)+\omega^2]}, \tag{8.6}$$

where we have also defined a wave-vector-dependent patch frequency

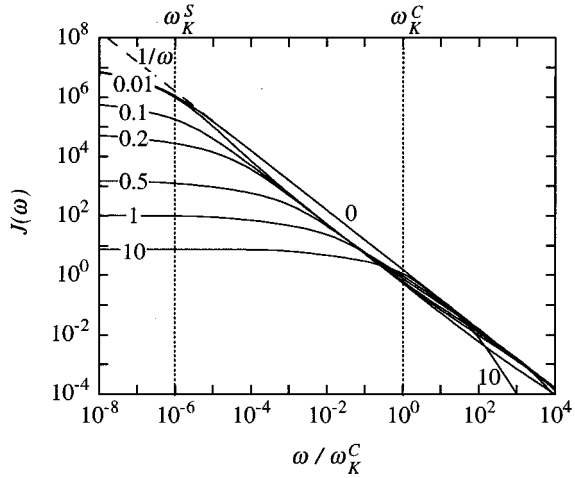

FIG. 14. Dispersion of the spectral density function $J(\omega)$, calculated from Eq. (8.6) with $\alpha=12$, $\delta=10^{-6}$, $N=10^4$, $\pi(\xi_K/a)^2 = \pi(d/a\sigma)^2 = 10^4/\sigma^2$, and σ as indicated. The plotted $J(\omega)$ has been reduced by $k_BT/(4\pi\kappa\omega_K^C)$. The dashed line corresponds to the $1/\omega$ dispersion in Eq. (7.22).

$$\Omega_K(\rho,\zeta)=\pi D_\perp(\rho,\zeta)/\xi_K^2. \tag{8.7}$$

In the fast-diffusion limit, $\Omega_K=\omega_K^S$, and the double integral can be performed analytically, yielding Eq. (7.16) when $\xi_K \gg a$, $\xi_B \ll L_\perp$, and $\omega \ll \omega_a$. In the general case, however, analytical efforts do not seem to give useful results. We therefore resort to numerical integration.

In Fig. 13, we compare the $J(\omega)$ dispersions in the fast- and slow-diffusion limits for the same value of $D_\perp^S+D_\perp^C$. Due to the effect of slow baroclinic modes, $J(0)$ is much larger and the dispersion starts at much lower frequency in the slow-diffusion limit. As expected, the two dispersion curves converge at high frequencies. Most interestingly, there is a power-law regime, $J(\omega)\sim 1/\omega^n$ with $n\approx 1$, that extends to much lower frequencies when diffusion is slow and baroclinic modes are responsible for the orientational fluctuations.

Figure 14 shows $J(\omega)$ dispersions for slow diffusion ($\delta=10^{-6}$) at variable coupling parameter σ. In the strong-coupling limit ($\sigma \gg 1$), the dispersion is much the same as in the fast-diffusion limit, but with $D_\perp^S$ replaced by $D_\perp^C$. In particular, we find a $1/\omega$ dispersion in the range $\omega_K^C \ll \omega \ll \omega_a$, with $\omega_K^C=\pi D_\perp^C/\xi_K^2$. The $1/\omega$ dispersion can be rationalized with the aid of Eq. (8.6), where the two factors in the integrand correspond to $\hat{H}(\mathbf{q})$ and $S(\mathbf{q},\omega)$. At a given frequency ω, $S(\mathbf{q},\omega)$ is dominated by modes with $\rho\Omega_K(\rho,\sigma)\approx\omega$. For $\omega \gg \omega_K^C$ and for strong coupling (so that $\Omega_K \approx \omega_K^C$), these are modes with $\rho \gg 1$. Since $\zeta \ll 1$, only transverse modes will then be given significant weight by $\hat{H}(\mathbf{q})$. The $1/\omega$ dispersion is thus produced by purely transverse modes (as if the system were two dimensional) of wavelengths shorter than ξ_K. At lower frequencies ($\omega<\omega_K^C$), $J(\omega)$ is affected by hydrodynamic interactions, reducing $J(0)$ by a factor $\frac{1}{2}$ (cf. Sec. VIII A). When $\sigma\to\infty$, Eq. (6.8) yields $\Omega_K=\omega_K^C(1+\zeta^2/\rho^2)$, showing that oblique modes can contribute for $\omega<\omega_K^C$.

For sufficiently weak membrane coupling, the $1/\omega$ regime is extended down to the diffusional patch frequency ω_K^S (cf. the uppermost curve in Fig. 14). Although $D_\perp^S \ll D_\perp^C$, it is now $D_\perp^S$ that sets the low-frequency cutoff for the $1/\omega$ dispersion. This happens because weakly coupled membranes fluctuate too slow to compete with molecular diffusion, which then also determines $J(0)$ (cf. Sec. VIII A). For moderately weak coupling, the $J(\omega)\sim 1/\omega^n$ dispersion deviates slightly from the strictly two-dimensional $1/\omega$ form: $n>1$ for $\omega<\omega_K^C$ whereas $n<1$ for $\omega>\omega_K^C$. For $\sigma \ll 1$, dynamic coupling effects are hardly manifested at all and $J(\omega)$ is essentially the same as in the fast-diffusion limit with $\pi(\xi_K/a)^2=\pi(d/a\sigma)^2$. (Note the difference in frequency scale between Figs. 10 and 14: $\omega_K^C=\omega_K^S/\delta$ and $\delta=10^{-6}$ here.)

ACKNOWLEDGMENT

This work was supported by grants from the Swedish Natural Science Research Council (NFR).

[1] L. D. Landau and E. M. Lifshitz, *Statistical Physics*, 3rd ed. (Pergamon, Oxford, 1980), Part 1.
[2] W. Helfrich, Z. Naturforsch. **30c**, 841 (1975).
[3] R. Lipowsky, Nature (London) **349**, 475 (1991).
[4] *Micelles, Membranes, Microemulsions, and Monolayers*, edited by W. M. Gelbart, A. Ben-Shaul, and D. Roux (Springer, New York, 1994).
[5] B. Halle and P.-O. Quist, J. Phys. (France) II **4**, 1823 (1994).
[6] B. Halle, Phys. Rev. E **50**, R2415 (1994).
[7] W. Kühner, E. Rommel, F. Noack, and P. Meier, Z. Naturforsch. **42a**, 127 (1987).
[8] E. Rommel, F. Noack, P. Meier, and G. Kothe, J. Phys. Chem. **92**, 2981 (1988).
[9] J. Struppe, Ph.D. thesis, Universität Stuttgart, 1996.
[10] M. Bloom and E. Sternin, Biochemistry **26**, 2101 (1987).
[11] J. Stohrer, G. Gröbner, D. Reimer, K. Weisz, C. Mayer, and G. Kothe, J. Chem. Phys. **95**, 672 (1991).
[12] E. J. Dufourc, C. Mayer, J. Stohrer, G. Althoff, and G. Kothe, Biophys. J. **61**, 42 (1992).
[13] K. Weisz, G. Gröbner, C. Mayer, J. Stohrer, and G. Kothe, Biochemistry **31**, 1100 (1992).
[14] G. Kothe and N. Heaton, in *Encyclopedia of Nuclear Magnetic Resonance*, edited by D. M. Grant and R. K. Harris (Wiley, Chichester, 1996), p. 4436.
[15] P. I. Watnick, P. Dea, and S. I. Chan, Proc. Natl. Acad. Sci. USA **87**, 2082 (1990).
[16] C. Dolainsky, A. Möps, and T. M. Bayerl, J. Chem. Phys. **98**, 1712 (1993).
[17] M. Bloom and T. M. Bayerl, Can. J. Phys. **73**, 687 (1995).
[18] R. Blinc, M. Luzar, M. Vilfan, and M. Burgar, J. Chem. Phys. **63**, 3445 (1975).
[19] J. A. Marqusee, M. Warner, and K. A. Dill, J. Chem. Phys. **81**, 6404 (1984).
[20] M. Bloom and E. Evans, in *Biologically Inspired Physics*, edited by L. Peliti (Plenum, New York, 1991), p. 137.
[21] F. Brochard and J. F. Lennon, J. Phys. (France) **36**, 1035 (1975).
[22] P. G. de Gennes and J. Prost, *The Physics of Liquid Crystals*, 2nd ed. (Clarendon, Oxford, 1993).
[23] F. Brochard and P. G. de Gennes, Pramana **1**, 1 (1975).
[24] W. Helfrich, Z. Naturforsch. **33a**, 305 (1978).
[25] W. Helfrich and R. M. Servuss, Nuovo Cimento D **3**, 137 (1984).
[26] P. G. de Gennes and C. Taupin, J. Phys. Chem. **86**, 2294 (1982).
[27] L. Golubovic and T. C. Lubensky, Phys. Rev. B **39**, 12 110 (1989).
[28] D. C. Morse and T. C. Lubensky, J. Phys. (France) II **3**, 531 (1993).
[29] N. Lei, C. R. Safinya, and R. F. Bruinsma, J. Phys. (France) II **5**, 1155 (1995).
[30] A. A. Kokin and A. A. Izmest'ev, Russ. J. Phys. Chem. **39**, 309 (1965).
[31] P. Brûlet and H. M. McConnell, Proc. Natl. Acad. Sci. USA **72**, 1451 (1975).

[32] A. Avogadro and M. Villa, J. Chem. Phys. **66**, 2359 (1977).
[33] G. Althoff, N. J. Heaton, G. Gröbner, R. S. Prosser, and G. Kothe, Colloids Surf. A **115**, 31 (1996).
[34] B. Halle, Liq. Cryst. **17**, 759 (1994).
[35] A. Abragam, *The Principles of Nuclear Magnetism* (Clarendon, Oxford, 1961), Chap. VIII.
[36] S. Gustafsson and B. Halle, Mol. Phys. **80**, 549 (1993).
[37] B. Halle, P-O. Quist, and I. Furó, Liq. Cryst. **14**, 227 (1993).
[38] D. M. Brink and G. R. Satchler, *Angular Momentum*, 2nd ed. (Clarendon, Oxford, 1968).
[39] B. Halle, in *Encyclopedia of Nuclear Magnetic Resonance* (Ref. [14]), p. 790.
[40] F. Noack, Prog. NMR Spectrosc. **18**, 171 (1986).
[41] J. S. Blicharski, Can. J. Phys. **64**, 733 (1986).
[42] S. Gustafsson and B. Halle, J. Chem. Phys. (to be published).
[43] F. C. Frank, Discuss. Faraday Soc. **25**, 19 (1958).
[44] P. G. de Gennes, J. Phys. (France) Colloq. **30**, C-65 (1969).
[45] A. Goetz, *Introduction to Differential Geometry* (Addison-Wesley, Reading, MA, 1970).
[46] B. Halle, J. Chem. Phys. **95**, 6724 (1991).
[47] M. Vilfan, M. Kogoj, and R. Blinc, J. Chem. Phys. **86**, 1055 (1987).
[48] R. Y. Dong, *Nuclear Magnetic Resonance in Liquid Crystals* (Springer, New York, 1994), Chap. 6.
[49] R. R. Vold and R. L. Vold, J. Chem. Phys. **88**, 4655 (1988).
[50] F. Brochard, J. Phys. (Paris) **34**, 411 (1973).
[51] J. H. Freed, J. Chem. Phys. **96**, 3901 (1992).
[52] S. Zumer and M. Vilfan, Phys. Rev. A **17**, 424 (1978).
[53] J. P. Hansen and I. R. McDonald, *Theory of Simple Liquids*, 2nd ed. (Academic, London, 1986).
[54] R. Holyst and A. Poniewierski, J. Phys. (France) II **3**, 177 (1993).
[55] G. Grinstein and R. A. Pelcovits, Phys. Rev. A **26**, 915 (1982).
[56] W. Helfrich, Z. Naturforsch. **28c**, 693 (1973).
[57] P. Canham, J. Theor. Biol. **26**, 61 (1970).
[58] D. Sornette and N. Ostrowsky, in *Micelles, Membranes, Microemulsions, and Monolayers* (Ref. [4]), Chap. 5.
[59] A. Caillé, C. R. Acad. Sci. B **274**, 891 (1972).
[60] L. Gunther, Y. Imry, and J. Lajzerowicz, Phys. Rev. A **22**, 1733 (1980).
[61] J. Als-Nielsen, J. D. Litster, R. J. Birgeneau, M. Kaplan, C. R. Safinya, A. Lindegaard-Andersen, and S. Mathiesen, Phys. Rev. B **22**, 312 (1980).
[62] F. C. Larche, J. Appell, G. Porte, P. Basserau, and J. Marignan, Phys. Rev. Lett. **56**, 1700 (1986).
[63] B. Halle, P.-O. Quist, and I. Furó, Phys. Rev. A **45**, 3763 (1992).
[64] J. M. Delrieu, J. Chem. Phys. **60**, 1081 (1974).
[65] G. J. Krüger, Phys. Rep. **82**, 230 (1982).
[66] P-Q. Quist and B. Halle, Phys. Rev. E **47**, 3374 (1993).
[67] M. S. Leaver and M. C. Holmes, J. Phys. (France) II **3**, 105 (1993).
[68] S. Gustafsson and B. Halle, J. Chem. Phys. **106**, 1880 (1997).
[69] B. Halle and S. Gustafsson, Phys. Rev. E **55**, 680 (1997).
[70] P. C. Martin, O. Parodi, and P. S. Pershan, Phys. Rev. A **6**, 2401 (1972).
[71] F. Nallet, D. Roux, and J. Prost, J. Phys. (France) **50**, 3147 (1989).
[72] R. Messager, P. Bassereau, and G. Porte, J. Phys. (France) **51**, 1329 (1990).
[73] S. Ljunggren, and J. C. Ericksson, J. Chem. Soc. Faraday Trans. **87**, 153 (1991).
[74] S. Ramaswamy, J. Prost, W. Cai, and T. C. Lubensky, Europhys. Lett. **23**, 271 (1993).
[75] S. Ramaswamy, J. Prost, and T. C. Lubensky, Europhys. Lett. **27**, 285 (1994).
[76] U. Seifert and S. A. Langer, Biophys. Chem. **49**, 13 (1994).
[77] C. Y. Zhang, S. Sprunt, and J. D. Litster, Phys. Rev. E **48**, 2850 (1993).
[78] D. Roux, C. R. Safinya, and F. Nallet, in *Micelles, Membranes, Microemulsions, and Monolayers* (Ref. [4]), Chap. 6.
[79] W. Cai and T. C. Lubensky, Phys. Rev. E **52**, 4251 (1995).
[80] T. C. Lubensky, J. Prost, and S. Ramaswamy, J. Phys. (France) **51**, 933 (1990).
[81] P. Pieruschka, S. Macelja, and M. Teubner, J. Phys. (France) II **4**, 763 (1994).
[82] E. van den Linden and F. M. Menger, Langmuir **9**, 690 (1993).
[83] *Handbook of Mathematical Functions*, edited by M. Abramowitz and I. A. Stegun (Dover, New York, 1970).
[84] B. Halle, H. Wennerström, and L. Piculell, J. Chem. Phys. **88**, 2482 (1984).
[85] B. Halle (unpublished).
[86] J. H. Freed, J. Chem. Phys. **66**, 4183 (1977).